University of Miskolc

Faculty of Earth Science and Engineering

Petroleum and Natural Gas Institute

Formation Susceptibility to Wellbore Instability and Sand Production in the Hajdúszoboszló field, Pannonian Basin: Hungary

(MSc Thesis)

Author's Name: Kolawole Oladoyin Olamuyiwa

Academic Advisor's Name: Dr. Kovácsné-Federer Gabriella

Industry Advisor's Name: Szabo Istvan

Miskolc, Hungary, April 2018

Institutional verification paper for thesis submit

for MSc students in Petroleum Engineering course

Student name: KOLAWOLE OLADOYIN OLAMUYIWA
Neptun-code: GYCNW8

Title of thesis: Formation Susceptibility to Wellbore Instability and Sand Production in the Hajdúszoboszló field, Pannonian Basin: Hungary

Originality statement

I, Kolawole Oladoyin Olamuyiwa hereby declare and certify with my signature under my criminal and disciplinary responsibility as the student of the Faculty of Earth Science and Engineering at the University of Miskolc that this thesis was my own work. I complied with the regulations of the Act LXXVI of 1999 on copyrights and with the requirements of thesis writing in the University. In the thesis only the references listed in the literature were used. Literal or reworded quotations have clearly been marked as references. I declare that the electronically uploaded and paper-based documents are concurrent. By signing this declaration, I acknowledge that the University of Miskolc refuses to accept the thesis and may initiate a disciplinary procedure against me if I am not the sole creator or an infringement of copyright in the thesis can be proved. Refusing to accept a thesis and initiating a disciplinary procedure is without prejudice to any other (civil, legal, criminal, legal) consequences of copyright infringement.

Miskolc, 03.05.2018

---

student signature

Statement of the Department Supervisor

I, the undersigned Dr. Kovacsne-Federer Gabriella, agree / ~~disagree~~ with the submitting of the thesis.[1)]
04.05.2018

---

signature of the Supervisor

Statement of the Industrial Advisor[2)]

I, the undersigned István Szabó, agree / ~~disagree~~ with the submitting of the thesis.[2)]
Szolnok, 26.03.2018

---

signature of the
Industrial Advisor

The thesis is submitted
Miskolc,

Administration of the Petroleum and
Natural Gas Institute

[1] The unchosen part should be marked with strikethrough. The thesis can be submitted with the disapproval of the Supervisor or the Industrial Advisor.
This verification paper with the necessary signatures must be attached in the original thesis after the thesis assignment.
[2] This paragraph can be erased in the absence of an Industrial Advisor.

Abstract

Wellbore instability and formation sand production pose potential risks for wellbore drilling, completion and production operations. In many sandstone reservoirs worldwide, sand production has been observed to accompany oil and gas production. In this study, we estimate, predict and quantify wellbore instability and sand production potentials in the Hajdúszoboszló field, Pannonian Basin, Hungary, using the Mechanical Earth Model (MEM). Our model relies on petrophysical log data obtained from an onshore gas well within the field as input data. Our model develops rock and sand failure mechanisms by estimating the rock elastic and strength properties, in-situ stresses and pore pressure of the reservoir rock with reference to the depth of stratigraphic column, from compressional slowness, shear slowness, density, porosity and shale volume. We adopted the 1-D MEM for our wellbore stability and sand production study of the Hajdúszoboszló field, because the model considered all available data to develop the rock mechanical properties, and also provide real-time numerical representation of the geomechanical state of the Hajdúszoboszló field in the Pannonian Basin. The 1-D MEM utilizes a workflow that involves, first, the creation of the mechanical stratigraphy of the reservoir rocks; second, the estimation of pore pressure, rock strength, rock elastic properties, and the horizontal stresses; third, wellbore stability analysis, where we developed mud weight profiles, wellbore shear failure and borehole breakdown; followed by sanding interval analysis for perforation completions. We further established the critical drawdown (CDDP) and critical reservoir pressure profiles for the suspected wellbore depth interval. Our results show the mechanical stratigraphy of unconsolidated sandstone and shale distribution in the reservoir, wellbore shear and tensile failures, wellbore breakout and breakdown pressures, wellbore sensitivity analysis, sanding interval analysis, critical drawdown pressure (CDDP) profile and sand failure zones. Based on careful observation of our results, we predict the wellbore intervals with high sand production potentials and wellbore instability within the reservoir formations. Therefore, we suggest significant wellbore failure during drilling process and also a high possibility of sand production into the wellbore during well completion at a formation interval of 550-937 m. Although there is need for data from additional wells in the field to be incorporated into our model prediction, we suggest that our preliminary model can be useful for critical decision making during drilling and completion operations across the Hajdúszoboszló field, Pannonian Basin, Hungary.

ACKNOWLEDGEMENTS

TABLE OF CONTENTS

LIST OF FIGURES

LIST OF TABLES

CHAPTER 1
INTRODUCTION

During the drilling process, the stress state in the vicinity of the wellbore is altered; thereby resulting in localised stress concentrations around the wellbore circumference. If the mud weight is insufficient, shear failure (breakout) of the wellbore walls can occur. This can take place in both weak and strong rocks depending on the overall stress regime, and magnitudes of the in-situ stresses (the principal stresses are assumed for modelling purposes to be vertical and horizontal). Typical problems that may arise include: tight spots, pack offs, high torque, caving noted at the shakers, a requirement for reaming and becoming stuck.

One of the oldest problems of oil and gas fields is sand production. It is usually associated with formations with shallow depth as compaction tends to increase with depth. It could also be encountered to a depth of 3658 m (12 000 ft) or more in some areas. Sand production erodes hardware, blocks tubulars, creates downhole cavities, and must be separated/disposed-off on the surface. Completion methods that allow sand-prone reservoirs to be exploited often severely reduce production efficiency. The challenge always faced is to complete wells, and at the same time keep formation sand in place without unduly restricting productivity.

In such challenging scenarios, it is highly recommended to carry out a Geomechanical study to predict the mud weight window in each section of the well. An Operable mud weight window shall be constrained on the lower side by the mud weight requirement to prevent rock shear failure or the kick whichever is higher and on the upper side by the maximum mud weight that formation can hold without experiencing any losses due to hydraulic fracturing.

Since sand control is generally an expensive investment for an oil/gas operator, it is of great interests for the operator to estimate if sand control is needed before production, or when sand control is needed after some time of sand-free production. To provide technical support for sand control decision-making, it is necessary to predict the production condition at which sand production occurs. The source of sand production is related to the unconsolidated grains of the formation or the rock failure during well bore drilling and perforation as well as hydrocarbon production. Accordingly, it is of great interest to estimate the critical conditions that the rock

failure occurs and sand migration is initiated. In practice, rock failure and sand production can be predicted either from the core laboratory experiments or evaluation of petrophysical logs as an in-situ method. The advantage of evaluation of rock elastic parameters to calculate the rock strength from logs is recognized as the real and original condition of the measurements. In addition, my study provides a platform for further investigation into wellbore stability and sanding analysis in other parts of the Pannonian Basin where available well data can also be incorporated in our model.

In this thesis, petrophysical well log data is used in combination with previous study results to estimate the potentials for wellbore instability and sand production within the Pannonian basin with emphasis on Hajdúszoboszló field in Hungary.

1.1. Thesis structure:

This thesis is divided into 5 chapters. Chapter two is an overview of the Rock Mechanical properties, in-situ stresses, wellbore stability and sand production studies. Chapter three presents the general geological, reservoir and petrophysical log information of the studied field located within the Pannonian Basin. It also explains the model workflow adopted as methodology adopted for this study. Chapter four pertains to estimated and observed results obtained from model evaluation of the studied formation. It also present the result discussions as it addresses the research aim. Finally in chapter five, final remarks including the final conclusions and recommendations for future studies are mentioned. Appendix A includes the MEM result for wellbore stability analysis. The SI metric conversion factors are listed in Appendix B.

CHAPTER 2

Background and Literature Review

2.1. Rock Mechanical Properties:

Rock mechanical properties, such as Poisson's ratio, shear modulus, Young's modulus, bulk modulus, and compressibility can be obtained from two different sources (Fjær et al. 2008):

(1) Laboratory measurements, which allow for direct measurements of strength parameters and static elastic behavior with recovered core material from discrete depths.

(2) Downhole measurements through wireline logging, which allow the determination of dynamic elastic constants from the continuous measurement of compressional and shear velocities.

Consequently, the mechanical properties obtained from laboratory core tests may be slightly or considerably different from those existing in-situ. Rock core alteration during and after drilling stage also may influence the geotechnical parameters (Taib and Donaldson 2004).

2.1.1. Stress and related concepts:

Stress is defined as a force per surface area through which the force is acting, as illustrated in Figure 2.1.

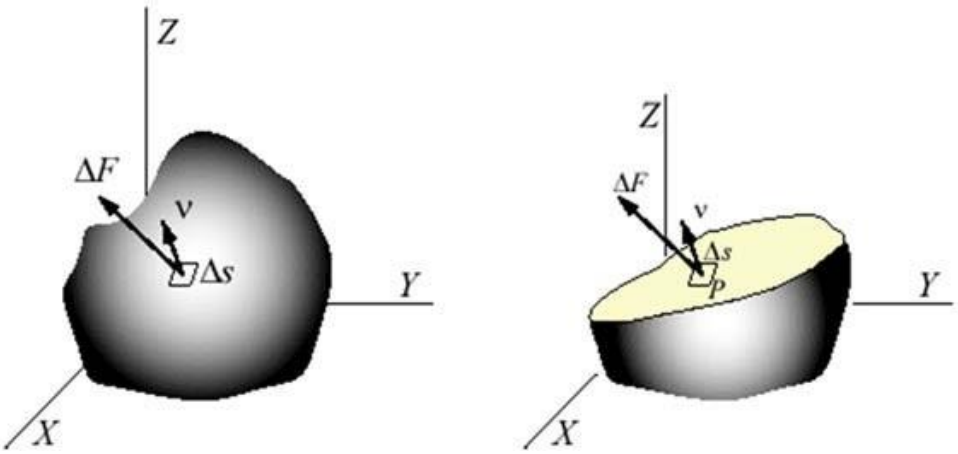

Figure 2.1: Force acting on the surface of body (Left); Force acting inside a solid (Right) (Mulders 2003).

Stress therefore can be interpreted as internal tractions that act on a defined internal plane.

Surface tractions or stresses acting on an internal datum plane, are typically decomposed into three mutually orthogonal components. One component is normal to the surface and represents normal stress. The other two components are tangential to the surface and represent shear stresses (Figure 2.2). The stress state at point P (Figure 2.2) can be represented with an infinite small cube with three stress components on each side of the cube.

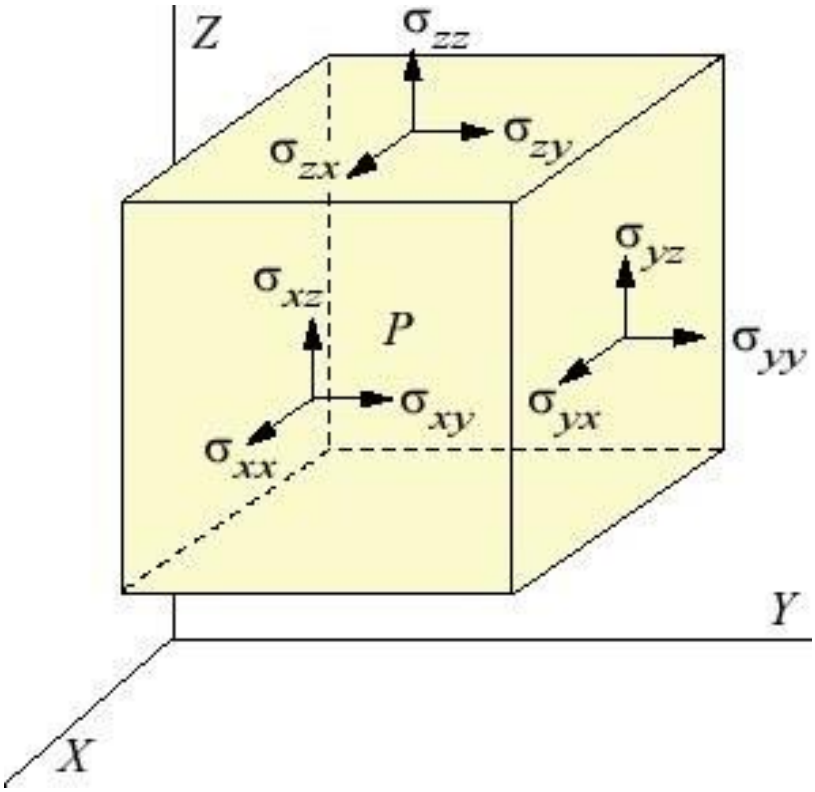

Figure 2.2: Stress vector components on coordinate planes (Mulders 2003).

2.1.2. Strain and related concepts:

Consider a bar with initial length L which is stretched to a length L_0. (The strain measure ε, a dimensionless ratio, is defined as the ratio of elongation with respect to the original length; the above strain measure is defined in a global perspective. The strain at each point may vary dramatically if the bar's elastic modulus or cross-sectional area changes (Angelov 2009).

$$\varepsilon = \frac{\Delta l}{l_o} \quad (1)$$

The components of strain for a solid like in the Figure 2.2 can be organized in a matrix similar to the stress tensor (Fjær et al. 2008):

$$\varepsilon = \begin{bmatrix} \varepsilon_{xx} & \varepsilon_{xy} & \varepsilon_{xz} \\ \varepsilon_{yx} & \varepsilon_{yy} & \varepsilon_{yz} \\ \varepsilon_{zx} & \varepsilon_{yz} & \varepsilon_{zz} \end{bmatrix} \quad (2)$$

The constitutive equations in mechanics are characterizing the behavior of specific materials. The relationship between internal stress and internal strain can be expressed as a constitutive equation (Tigrek, 2004). The mechanical behavior of real materials is very diverse and complex and it would be impossible to formulate equations which are capable of determining the stress in a body under all circumstances (Spencer, 2004).

The aim is to establish equations which describe the most important features of the behavior of the material in a given situation. Such equations could be regarded as defining ideal materials. One ideal model is based on the assumption of a linear relation between stress and strain which will lead to a linear constitutive equation. The common effect of different strain histories will be equal to the sum of the effects of the individual strain histories. For a locally reacting material the internal stress at a certain fixed position can be related entirely to the strain history of that local material (Tigrek 2004).

Materials following the same constitutive equations are building one rheological class. Depending on the material properties and stress/strain relation the rheological classes can be elasticity, plasticity, or viscosity. In our case study we will discuss only the case of elasticity. Elastic behavior is characterized by the following two conditions (Mase 1999):

(1) The stress in a material is a unique function of strain.
(2) The material has the property of complete recovery to a “natural” shape upon removal of applied forces.

The behavior of a material can be elastic or not elastic (inelastic). Elastic behavior means that applied stress leads to a strain, which is reversible when the stress is removed.

However, the linear elasticity is simple, and the parameters required can be estimated from log data and standard laboratory tests. The rocks in the upper lithosphere can be considered elastic for loads with a duration that is short when compared with the age of the Earth (Ranalli 1995). This gives us the ability to consider elasticity as the most important rheological class in geo-mechanical modeling (Tigrek 2004).

2.1.3. The Mohr–Coulomb criterion:

If a piece of rock is subject to sufficiently large stresses, a failure will occur. This implies that the rock changes its shape permanently, and possibly also falls apart. The condition is accompanied with a reduced ability to carry loads. Rock failure is an important phenomenon also for petroleum related rock mechanics, as it is the origin of severe problems such as borehole instability and solids production. It is therefore useful to be able to predict under which conditions a rock is likely to fail (Fjær et al. 2008; Taib and Donaldson 2004).

A more general and frequently used criterion is the Mohr–Coulomb criterion, which is based on the assumption that $f(\sigma')$ is a linear function of σ':

$$|\tau| = S_o + \mu\sigma' \tag{3}$$

Where:

μ = Coefficient of internal friction

S_o = Inherent shear strength

τ = Shear stress

σ' = Normal stress

In Figure 2.3 we can draw the Mohr–Coulomb criterion, and show a Mohr's circle that touches the failure line. The angle ϕ defined in the Figure is called the angle of internal friction (friction angle) and is related to the coefficient of internal friction by:

$$tan\emptyset = \mu \tag{4}$$

Where:

μ = Coefficient of internal friction

Ø = Angle of internal friction (Friction Angle)

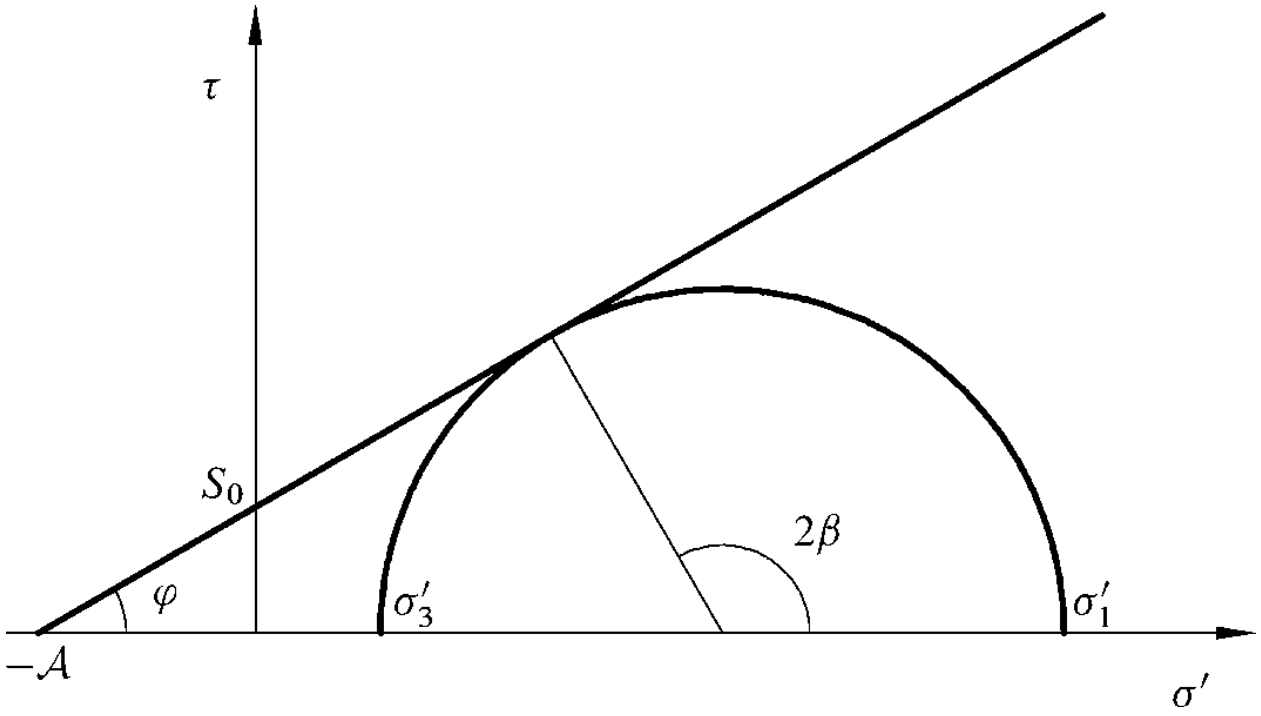

Figure 2.3: Mohr–Coulomb criterion in τ– σ' space (Fjær et al. 2008)

The allowable range for ϕ is from 0° to 90° (in practice the range will be smaller, and centered on approximately 30°), hence it is clear that β may vary between 45° and 90°. It is concluded that the failure plane is always inclined at an angle smaller than 45° to the direction of σ' Fig.2.4 shows schematically how the failure planes may be oriented in a rock described by the Mohr–Coulomb criterion. One important point to note is that β is given solely by ϕ, which is a constant in the Mohr–Coulomb criterion. Thus the orientation of the failure plane is independent of the confining stress. This is a special feature for the Mohr–Coulomb criterion. Experiments often show that the failure angle decreases with increasing confining pressure, in particular at low confining pressures (Fjær et al. 2008).

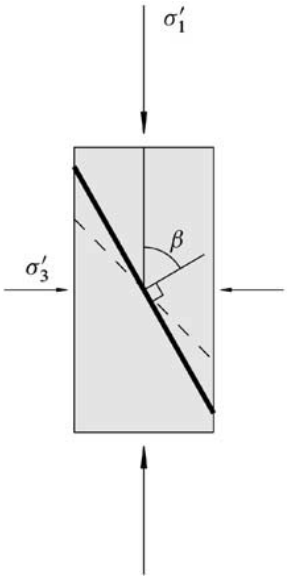

Figure 2.4: Orientation of the failure plane relative to the largest principal stress. (The thick solid line shows the failure plane for a friction angle of 30°. The dashed line shows the maximum inclination of the failure plane relative to σ'_1, according to the Mohr–Coulomb criterion) (Taib and Donaldson 2004).

2.2. Rock Strength:

Strength is the ability of rock to resist stress without yielding or fracturing (Fjær et al. 2008). It is influenced by the mineralogy of the rock particles and by the character of the particle contacts (Taib and Donaldson 2004). Figure 2.5 illustrates a typical test specimen, a cylinder with length to diameter ratio 2:1. An (axial) stress to the end faces of the cylinder, while a confining oil bath provides a stress of possibly different magnitude to the circumference (Fjær et al. 2008). If the confining stress is zero, the stress is uniaxial stress test (also called unconfined compression test). When the test is performed with a non-zero confining pressure, a so-called triaxial test is performed. Uniaxial compressive strength tests are used to determine the ultimate strength of a rock, i.e., the maximum value of stress attained before failure. The uniaxial strength is one of the simplest measures of strength to obtain These properties are the result of the various processes of deposition, diagenesis, and catagenesis that formed the rock, later modified by folding, faulting, fracturing, jointing, and weathering. Consequently, the strength of rocks reflects their geological

history (Taib and Donaldson 2004). Rock strength is estimated from two common laboratory techniques: uniaxial compressive strength tests, and triaxial or confined compressive strength tests. Uniaxial compressive strength (UCS) tests are used to determine the ultimate strength of a rock, i.e., the maximum value of stress attained before failure.

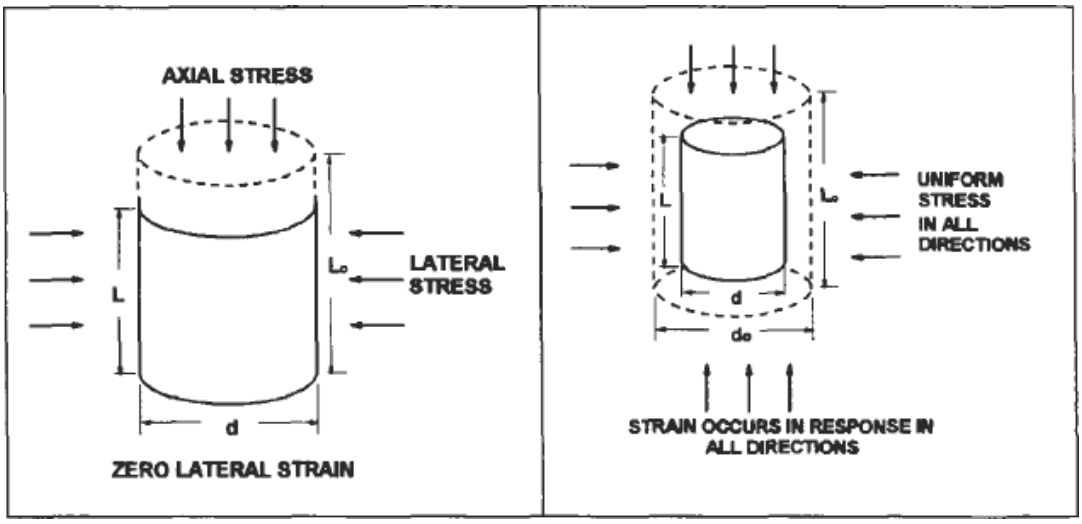

Figure 2.5: Typical samples for Uniaxial or Triaxial tests (Taib and Donaldson 2004)

The uniaxial strength is one of the simplest measures of strength to obtain. Its application is limited, however, and it is generally used only when comparisons between rocks are needed.

Uniaxial compression tests are influenced by several factors: size and shape of the test sample, rate of loading, amounts and types of fluid present in the rock sample, mineralogy, grain size, grain shape, grain sorting, and rate of loading (Taib and Donaldson 2004):

1. The length-to-diameter ratio, also called the slenderness ratio, of the rock sample should be approximately 2 to 1.
2. The ends of the sample should be parallel and ground flat to within 0.025 mm; otherwise, low values of compressive strength are obtained.
3. Size effects are considerable only if flaws exist in the rock sample: The larger the sample, the greater the probability of a flaw existing in the sample. Size effects can be reduced by testing a large number of samples with the same size and calculating the average,

preferably the geometric mean, of compressive strength values.

4. Because fluid content could reduce the compressive strength, it is recommended to perform the uniaxial test under fluid saturations similar to those existing in the reservoir. Reduction in compressive strength due to the presence of fluids could occur in several ways. It is probable; however, that in many rocks the effect of pore pressure is the main cause of reduction in rock strength. The pore pressure could affect the intergranular contact stresses and cause instability along a weakness plane.
5. High rates of loading should be avoided, as they tend to yield abnormally high compressive strength values. Loading rates in the range of 0.5 MPa/s to 3 MPa/s are considered normal and generally cause negligible change in compressive strength of rock samples.

Uniaxial test in Figure 2.6 has been shown for typical test. The applied axial stress (denoted σ_z) is plotted as a function of the axial strain (ε_z) of the sample. In elastic region the rock deforms elastically. If the stress is released, the specimen will return to its original state. After Yield point, the point beyond which permanent changes will occur. The sample will no longer return to its original state upon stress relief.

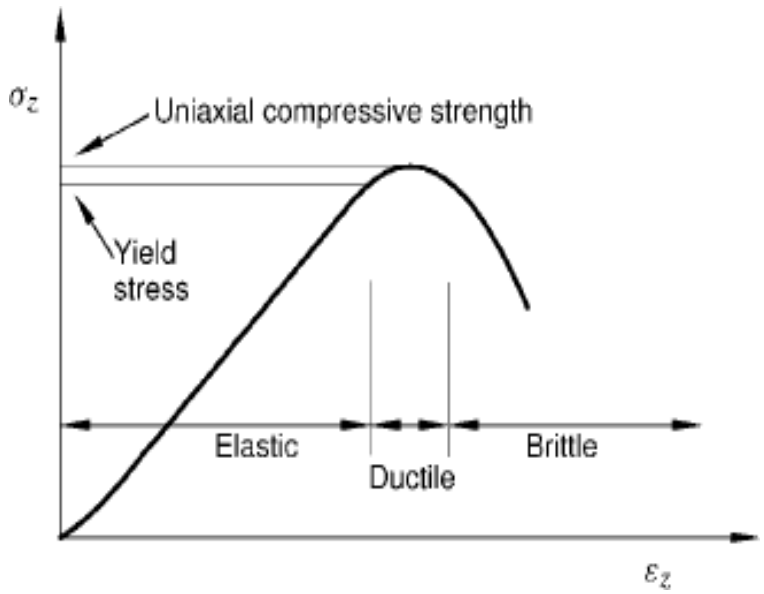

Figure 2.6: Principle sketch of stress versus deformation in a uniaxial compression test Fjær et al. 2008).

At Uniaxial compressive strength, the peak stress. In ductile region**,** the sample undergoes permanent deformation without losing the ability to support load. In brittle region**,** the specimen's ability to withstand stress decreases rapidly as deformation is increased (Fjær et al. 2008). The relationship between stress and strain is commonly expressed in graphs known as stress-strain diagrams. The rock in Figures 2.7 and 2.8 is under compression. With increasing stress the specimen becomes shorter, and the strain (deformation) is plotted in terms of the percentage of shortening of the rock sample. Curve A represents a typical behavior of a brittle rock, which deforms elastically up to a stress of approximately 20,000 psi (137.9 MPa), shortening 0.5% before rupture. Curve B describes an ideal plastic substance. First it behaves elastically until reaching the proportional elastic limit, which is the point at which the curve departs from the straight line. Then the rock deforms continuously with any added stress.

Curves C and D can represent the more typical plastic behavior of the rock. Once the elastic limit is reached, rock sample C becomes progressively more difficult to deform. With increased stress, rock sample D reaches its ultimate strength point, beyond which less stress is necessary to continue the deformation until rupture. The mechanical behavior of rocks is controlled not only by their inherent properties, e.g., mineralogy, grain size, porosity, width and density of fractures, etc., but also confining pressure, temperature, time, and interstitial fluids. It is evident that the strength of the rock increases with confining pressure. Such experiments indicate that rocks exhibiting very little plastic deformation near the surface of the earth may be very plastic under high confining pressure (Taib and Donaldson 2004).

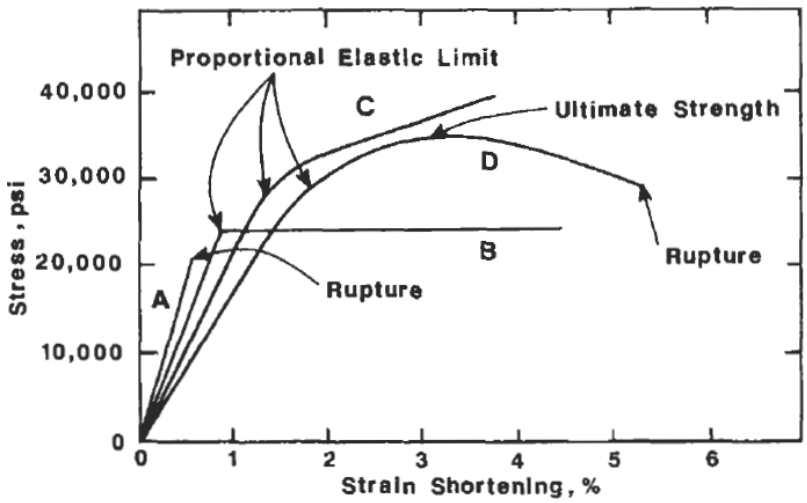

Figure 2.7: Relationship between Stress-strain (Taib and Donaldson 2004)

Thus, under a confining pressure of 1,000kg/cm2 or greater, limestone will deform plastically.

Heating particularly enhances the ductility-that is, the ability to deform permanently without loss of cohesion-of calcareous and evaporate rocks; however, it has little effect upon sandstones. Much rock deformation takes place while solutions capable of reacting chemically with the rock are present in the pore spaces. This is notably true of metamorphic rocks, in which extensive or complete recrystallization occurs.

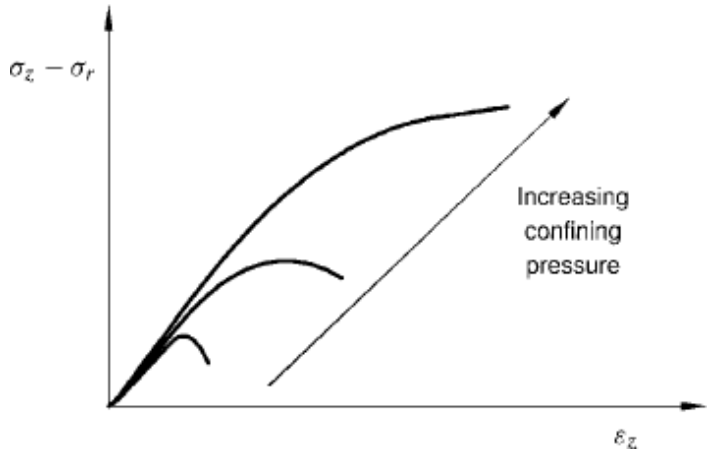

Figure 2.8: Triaxial testing: typical influence of the confining pressure on the shape of the differential stress (axial stress minus confining pressure) versus axial strain curves (Fjær et al. 2008).

A triaxial test is usually performed by increasing the axial and confining loads simultaneously, until a prescribed hydrostatic stress level is reached. The axial loading is normally applied such that it gives a constant axial deformation rate. The most common mode of failure observed in uniaxial and triaxial tests is shear failure. This failure mode is caused by excessive shear stress.

Another failure mode is tensile failure, which is caused by excessive tensile stress. Finally, pore collapse is a failure mode that is normally observed in highly porous materials, where the grain skeleton forms a relatively open structure. Pore collapse is usually caused by excessive hydrostatic stress (Fjær et al. 2008).

2.3. Tensile Failure:

Tensile failure is occurring if the effective tensile stress across some plane in the sample exceeds a critical limit. This limit is called the tensile strength; it is given the symbol T_0, and has the same unit as stress (Taib and Donaldson 2004). The tensile strength is a property of the rock. Sedimentary rocks have a rather low tensile strength, typically only a few MPa or less. In fact, it is a standard approximation for several applications that the tensile strength is zero. A sample that suffers tensile failure typically splits along one or very few fracture planes, as illustrated in Figure 2.9. The fracture planes often originate from preexisting cracks oriented more or less normal to the direction of the tensile stress. The highest probability of damage for the rock is at the perimeter of the largest of these cracks; hence the largest crack(s) will grow increasingly faster and rapidly split the sample. The tensile strength is sensitive to the presence of cracks in the material. The failure criterion, which specifies the stress condition for which tensile failure will occur, and identifies the location of the failure surface in principal stress space, is given as (Fjær et al. 2008):

$$\sigma = -T_o \tag{5}$$

Where:

T_o = Tensile strength

σ = Stress

Perkins and Weingarten (1988) studied the conditions necessary for stability or failure of a spherical cavity in unconsolidated or weakly consolidated rock. Weigarten and Perkins derived an equation describing tensile failure condition in terms of pressure drawdown, wellbore pressure, formation rock cohesion and frictional angle.

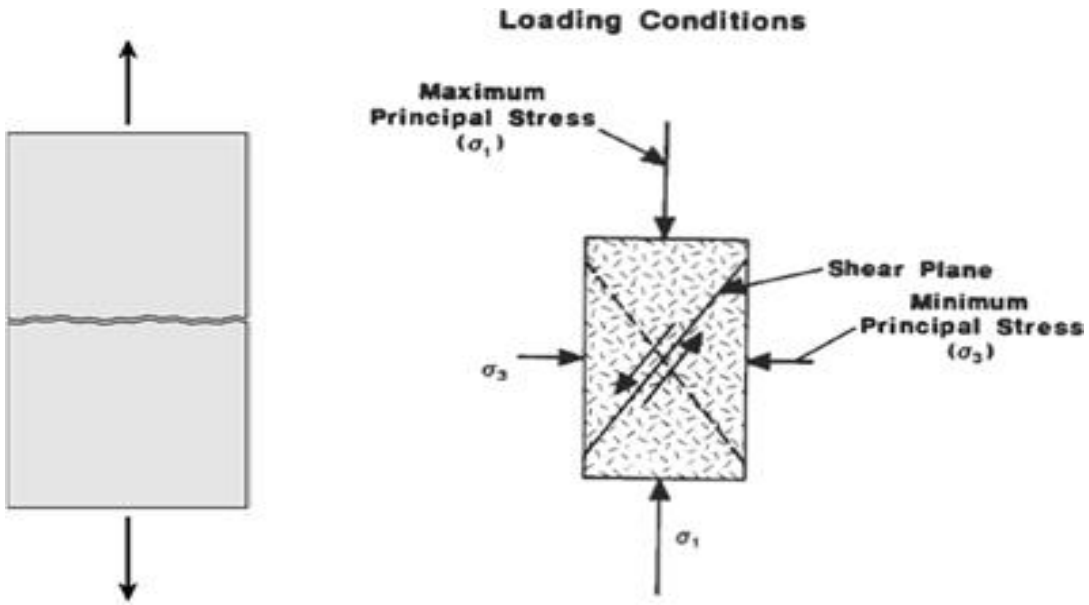

Figure 2.9: Tensile and shear failure (Fjær et al. 2008; Taib and Donaldson 2004)

2.4. Shear Failure:

Shear failure occurs when the shear stress along some plane in the sample is sufficiently high. Eventually, a fault zone will develop along the failure plane, and the two sides of the plane will move relative to each other in a frictional process, as shown in Fig. 2.10. It is well known that the frictional force that acts against the relative movement of two bodies in contact depends on the force that presses the bodies together. It is therefore reasonable to assume that the critical shear stress (τ_{max}) for which shear failure occurs, depends on the normal stress (σ') acting over the failure plane. Given as (Fjær et al. 2008; Taib and Donaldson 2004):

$$|\tau_{max}| = f\,(\sigma') \qquad (6)$$

Where:

τ_{max} = Critical Shear stress

σ' = Normal stress

This assumption is called Mohr's hypothesis. In the τ–σ' plane, Eqn. (6) describes a line that separates a "safe region" from a "failure" region. Eqn. (6) can be considered as a

representation of the failure surface in the τ–σ' plane. This line is sometimes referred to as the failure line or the failure envelope. An example is shown in Fig. 2.10, where we have also indicated the three principal stresses and the Mohr's circles connecting them. The stress state of Fig. 2.10 represents a safe situation, as no plane within the rock has a combination of τ and σ' that lies above the failure line. Assume now that σ'_1 is increased. The circle connecting σ'_1 and σ'_3 will expand, and eventually touch the failure line. The failure criterion is then fulfilled for some plane(s) in the sample, and the sample fails. Note that the value of the intermediate principal stress (σ'_2) has no influence on this situation. Since σ'_2 by definition lies within the range (σ'_3,σ'_1), it does not affect the outer of Mohr's circles, and hence it does not affect the failure (Fjær et al. 2008; Taib and Donaldson 2004).

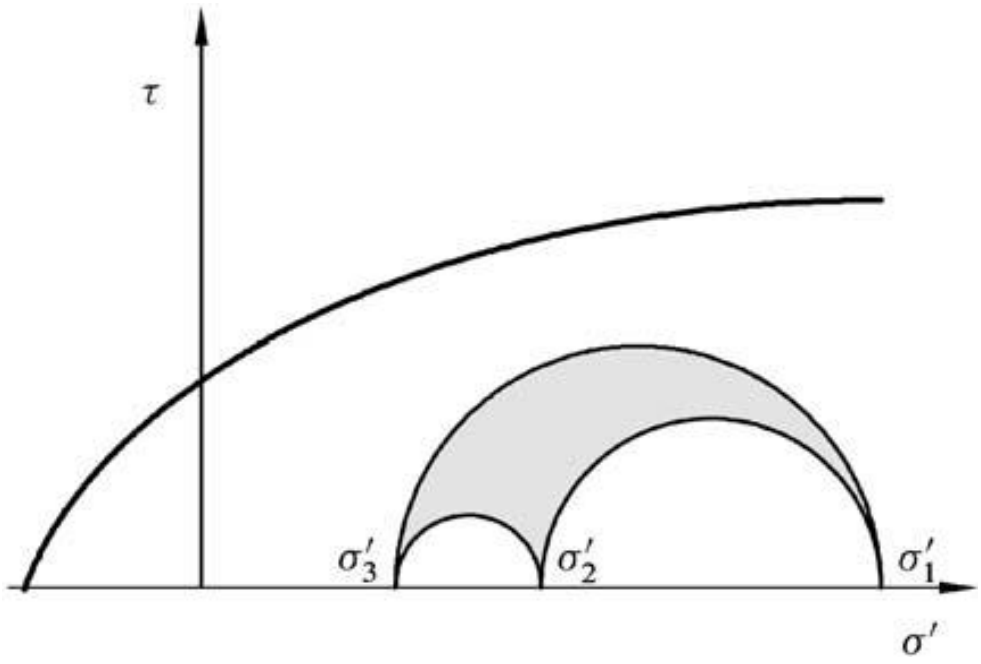

Figure 2.10: Failure curves as specified by Eq. (6), in the shear stress-normal stress diagram (Fjær et al. 2008; Taib and Donaldson 2004).

Several rock strength criteria have been employed to predict well bore stability and sand production in the literature. Laboratory tests may be necessary to know which strength criterion best describes the behavior of the rock studied. Among those strength criteria, the Von Mises criterion is used more in metal than in porous media, the Mohr Coulomb and Hoek- Brown criteria consider only the effect of maximum and minimum principal stresses while the Drucker-Prager, Modified Lade and Modified Weilbols & Cook criteria involve also intermediate principal stress (EI-Sayed 1991). The systematic comparison of the use of all those criteria has not been made. For rock behaves in the brittle regime, the sand production criterion may be the same as the rock strength criterion.

However, for rock behaves in the ductile regime, it may be necessary to simulate the post yield behavior (hardening or softening) and to propose some other sand production criterion. Thus, pure shear failure, as defined by Mohr's hypothesis, depends only on the minimum and maximum principal stresses and not on the intermediate stress.

By choosing specific forms of the function $f(\sigma')$ of Eq. (6), various criteria for shear failure are obtained. The simplest possible choice is a constant. The resulting criterion is called the Tresca criterion. The criterion simply states that the material will yield when a critical level of shear stress is reached (Fjær et al. 2008; Taib and Donaldson 2004):

$$\tau_{max} = 12\,(\sigma_1' - \sigma_3') = S_o \qquad (7)$$

S_o is the inherent shear strength (also called cohesion) of the material. In a Mohr τ–σ' plot the Tresca criterion appears simply as a straight horizontal line.

2.5. Horizontal Stress Direction:

Determination of horizontal stress directions is based on the possibility of failure at the borehole wall which can be detected by borehole logging tools. To be detectable, the failures must occur in the period after drilling and prior to logging. In a vertical borehole which penetrates layers of significantly different horizontal stresses ($\sigma_H > \sigma_h$), two distinct failure modes can be detected: compressive and tensile failure. The directions of these two failure modes in an idealized situation are uniquely given by the directions of the two principal horizontal stresses, as

illustrated in Figure.2.11 Compressive failure or shear failure will be induced in the direction parallel with the smallest horizontal stress (σ_h) if the well pressure is low enough to induce shear failure. This is commonly referred to as. Tensile failure will occur in the direction parallel with the largest horizontal stress (σ_H) if the well pressure is large enough to induce fracturing. Note that in situations with large variations in equivalent circulating density (ECD) of the drilling fluid it may be possible to observe both failure modes at the same depth. Once a failure has occurred on the borehole wall, it is tempting to try to back-calculate also stress magnitudes, especially the magnitude of the largest horizontal stress by using elastic theory and appropriate failure criteria.

However, a number of assumptions are required for such analyses, rendering the results uncertain. Such estimates can at best be considered upper or lower bounds on the stress magnitudes. The large amount of information that can be acquired by new tools, such as the Sonic Scanner, may eventually reduce some of the uncertainty, and allow for more reliable estimation of the in-situ stresses.

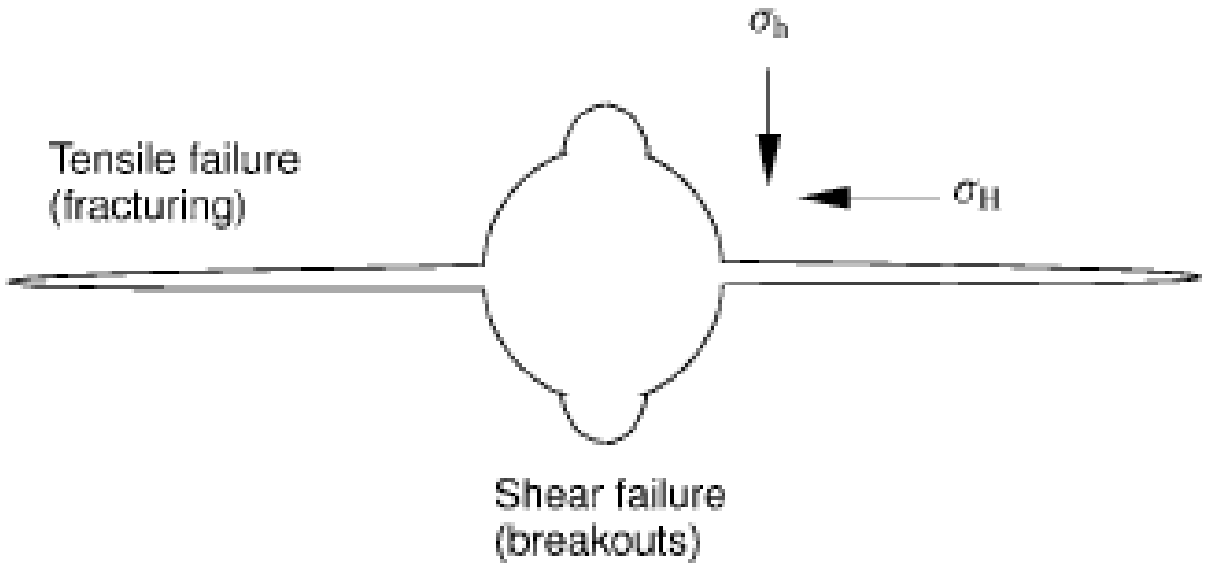

Figure 2.11: Illustration of directions for compressive and tensile failure around a vertical borehole (Fjær et al. 2008).

2.6. Wellbore Instability:

Wellbore instability occurs as a result of excessive stress concentrations around the wall of a borehole often induced by inadequate mud support during drilling operations (Qiuguo et al., 2013). The earth's in-situ stresses are caused by overburden weight, tectonic forces and pore pressure. Geomechanical model for wellbore analysis is of utmost importance for a successful drilling program (Plumb et al., 2000) and field development plans. This geomechanical study is also important because of its adverse effects on drilling performance, and also it's potential to severely impact on both drilling schedule and budget (Wu et al., 2006). Due to the presence of overpressured formations in the Pannonian Basin, wellbore instability is often experienced. Exploration drilling is extremely risky in the Pannonian Basin, and this can easily cause wellbore failure and blowouts (Alliquander and Csaba, 1976).

In this study, we assess the wellbore stability in the Hajdúszoboszló field of the Pannonian Basin. In Hungary, oil and gas prospecting, exploration and production activities are more than 70 years old in Hungary. The Hungarian Paleogene reservoir is made up of one gas field and one oil field in excess of 1 million barrels of oil equivalent (MMBOE), along with other six smaller fields (Dolton, 2006). During this period in Hungary, we have recorded 73 documented blowouts and more undocumented kicks (Szabo, 2001). A typical example is the Shallow gas blowouts (Szabo, 2001) in the Hajdúszoboszló field, Hungary, which resulted in the total loss of the rig. Abnormally high temperatures and the extreme overpressures of the unconsolidated formations have been identified as the cause of wellbore instability and failure in the Pannonian Basin, Hungary (Szabo, 2001). This, in addition to the availability of well data, is the reasons why we attempt to predict and avoid wellbore instability in the Hajdúszoboszló field.

During wellbore drilling process, stresses are induced and distributed in the formations that surround the well. As discussed by Szabo (2001), the thick and unconsolidated formations in Hajdúszoboszló field are under tensile and shear stresses, and tend to fracture vertically, this may cause borehole shear stresses to exceed its strength and bring about a stress-induced wellbore failure. Wellbore instability may have resulted in the blowout at the Hajdúszoboszló field, which may be encountered due to low fracture gradients at shallow depths (Szabo, 2001). In Szabo, 2001, at depths below 1889 m (6200 ft), the formations are locally exposed to overburden pressures of over 50-60% of normal formation pressures, and they exhibit relatively extreme temperature values of over 170 ^{o}C (338 ^{o}F) (Alliquander, 1970). According to Alliquander

(2001) and Szabo (2001), for most reservoir fields in Hungary, the cases of wellbore instability recorded shows large wellbore failure occurring at depths of 191.92-304.8 m (400-1000 ft), below 1981 m (6500 ft). The wellbore failures recorded also occur with pressure gradients of 20.3585–21.4896 kPa/m (0.9-0.95 psi/ft), which is far above the normal hydrostatic pressure gradients of 10.6317–10.8579 kPa/m (0.47-0.48 psi/ft) (Alliquander, 2001; Szabo, 2001). Previous application of wellbore stability models (Anderson et al., 1973; Bradley, 1979; Bell. and Gough, 1979; Zoback et al., 1985; Plumb and Hickman, 1985; McClean and Addis, 1990; Charlez and Heugas, 1991; Bradford and Cook, 1994) encountered severe wellbore instability problems while drilling in high-risk wells.

Mechanical Earth Model (MEM) has been identified as one of the most valuable models for wellbore stability analysis of various fields across the world (Plumb et al., 2000; Van Den Hoek et al., 1996; Papanastasiou, 2006).

2.7. Sand Production:

Sand production into a borehole (sanding) is a long-standing problem in drilling operations as it affects well productivity and equipment (Subbiah et al., Ispas et al., 2002; Zhou and Sun, 2016). Sand production can be categorized into three types based on the observed sand production features during oil and gas production: unstable sand production, continuous sand production, and catastrophic high-rate sand production (Zhou and Sun, 2016; Ispas et al., 2002).

The mechanism of sand production is very complicated, and sand production can occur during drilling, completion, production, or injection processes. If the problem of sand production is not handled properly, sand production will continue to increase and thereby affects the development of oil and gas fields. Problem caused by sand production includes (Zhou and Sun, 2016): lower production rates, damage of the downhole equipment and surface facilities, formation collapse, production decline, abandonment of wells, abrasive corrosion of pipes, blocking pipes, production interval being buried by sand production. Cost of artificial lift, gathering and transportation, and also the supported facilities to dispose wastes, will also increase due to sand production.

Approximately 70% of the world's oil and gas resources are present in poorly consolidated sandstone reservoirs (Zhou and Sun, 2016). Unconsolidated reservoirs are distributed in nearly every oilfield around the world, which includes (Zhou and Sun, 2016):

Wilmington Oilfield and Kern River Oilfield in California, Bell Creek Oilfield in Montana, S.E. Paul's Valley Oilfield in Oklahoma, Cold Lake and Elk Point in Canada, and some Paleogene-Neogene reservoirs in Indonesia, Trinidad, and Venezuela. Hajdúszoboszló field in Hungary also belong to the group of unconsolidated reservoirs. One common feature of all these reservoirs is a shallow depth, usually less than 1800 m (5900 ft) (Zhou and Sun, 2016). These shallow-depth reservoirs have poor cementation and high porosity (usually greater than 25%).

In poorly consolidated formations, sand production may be triggered which detaches the sand grains and carry them into the wellbore. This effect grows with higher flow rate and with high pressure differentials during drawdown. During perforation, permeability around the surface of a perforation cavity may be reduced, which weakens the formation, and with any sudden change in flow rate, wellbore failure will likely occur leading to production of solids (Carlson et al., 1992). Water influx can also cause sand production by reducing the capillary pressure between sand grains. In Hungary, poorly consolidated formations with abnormal pressure that have possibility of sand production into the wellbore become increasingly frequent in the range of depth below 1890 m (6200 ft) (Szabo, 2001).

With the increasing demand of petroleum worldwide, and unstable oil prices after a global fall in oil prices, under such situation, major oil producing countries and petroleum corporations are beginning to focus on trying to reduce production costs and also improve production rate of oil and gas fields. In order to enhance oil and gas production rate, higher drawdown becomes necessary. In this study, we assess the potential for sand production in the Hajdúszoboszló field of the Pannonian Basin. Hungary, centrally located in the Pannonian Basin, is one of the primary target of petroleum exploration in the province due to its approximately 2.3 billion barrels of oil and 13 Trillion cubic feet gas production from thousands of wells drilled over the last 75 years (Bada and Tari, 2012). Careful predictions of reservoir intervals that are susceptible to sand production are therefore critical for efficient production of the field's hydrocarbon reserve. Here, we identify specific intervals within the known reservoir formations in the Hajdúszoboszló field that pose the greatest potential for sand production.

Among the published articles on sand production predictions (Van Den Hoek et al., 1996; Willson et al., 2002; Ispas et al., 2002; Acock et al., 2004; Franquet et al., 2005; Wu et al., 2006; Papanastasiou, 2006; Mohiuddin et al., 2009; Ranjith et al., 2013; Al-Shaaibi et al., 2013; Subbiah et al., 2014; Amiebenomo et al., 2015; Zhou and Sun, 2016; Isehunwa et al., 2017),

some of the common methods used to predict sand production are: the BP sanding model, the Mechanical Earth Model (MEM), polyaxial cell laboratory experiment, and erosional failure mechanism concept.

CHAPTER 3

Data and Methods

In this chapter, the field data and geologic characteristics of a single on-shore gas well (HSZ-197) is used for petrophysical analysis and geomechanical prediction of wellbore instability and sand production, and it is located in the Hajdúszoboszló field (Figure 3.1a), Pannonian Basin, Hungary.

3.1. Geologic Background of Hajdúszoboszló field:

The Pannonian Basin (Figure 3.1a) located in Central European Province is occupied majorly by Hungary (center), Croatia, Romania and Serbia-Montenegro (formerly Yugoslavia). The Pannonian Basin was evolved in the Neogene age, 23 to 2.5 million years ago (Ma) (Bada and Tari, 2012). The Pannonian Basin tectonic configuration (Figure 3.2) is made up of a major system of Cenozoic basins superimposed on inner elements of highly deformed and complexly faulted nappes of Mesozoic, Paleozoic, and Precambrian rocks of the Alpine-Carpathian fold belt. The Pannonian Basin is composed of a complex system of extensional sub-basins joined together by a far-reaching younger Neogene and Quatemary sediment fill (Dolton, 2006). The hydrocarbon formation in Hungary is of Neogene age, predominantly covered by Pliocene and Miocene formations with Oligocene formation overlying them (Alliquander and Csaba, 1976). The base rocks found in Hungary includes but not limited to: Oligecene shale, Mesozoic carbonated fissured rocks, dolomites, Miocene sandy formations and Pliocene sandstones (Dolton, 2006). In the lower-Pliocence (the lower-Pannonian Basin), the formations occur under excessive (95%) overpressure (Alliquander, 1970).

In Hajdúszoboszló field located within the Hungarian Pannonian Basin, lies the NE-SW-trending Szolnok Paleogene Flysch zone (Figure 3.2), which is strongly deformed and offers both source and reservoir rocks with a variety of lithology (Bada and Tari, 2012). Previous studies on the Pannonian basin confirmed the presence of over-pressured, weak, unconsolidated formations in the basin, and suggested the potential for sand production into the wellbore during oil and gas production (Dolton, 2006; Bada and Tari, 2012; Alliquander and Csaba, 1976; Alliquander, 1970; Szabo, 2001). The geological configuration of the Pannonian Basin, Hungary, has revealed the following: significant overpressured formations, in-situ temperature conditions

considerable higher than the global average, and the formation fracturing pressure irregularities (Szabo, 2001).

The Hajdúszoboszló field is an interesting area in Hungary. The Hajdúszoboszló field is confined primarily to Oligocene sands inter-fingering with shale, and the hydrocarbon generation in this field took place during the last 10 Ma (Bada and Tari, 2012). The Hajdúszoboszló field has some special tectonic features: in the upper section of the sequence of strata, the minimum principal horizontal stress (Figure 3.1b) lie in the East-North-East to West-South-West direction (Szabo, 2001). The fracture gradient in the field hardly exceeds 0.1583 bar/m (0.7 psi/ft) (Szabo, 2001). As a result of these features, the reservoir formations in the Hajdúszoboszló field fail very easily, and the resultant overburden stress develops up to the surface, thereby causing wellbore instability and sand production in the field (Szabo, 2001).

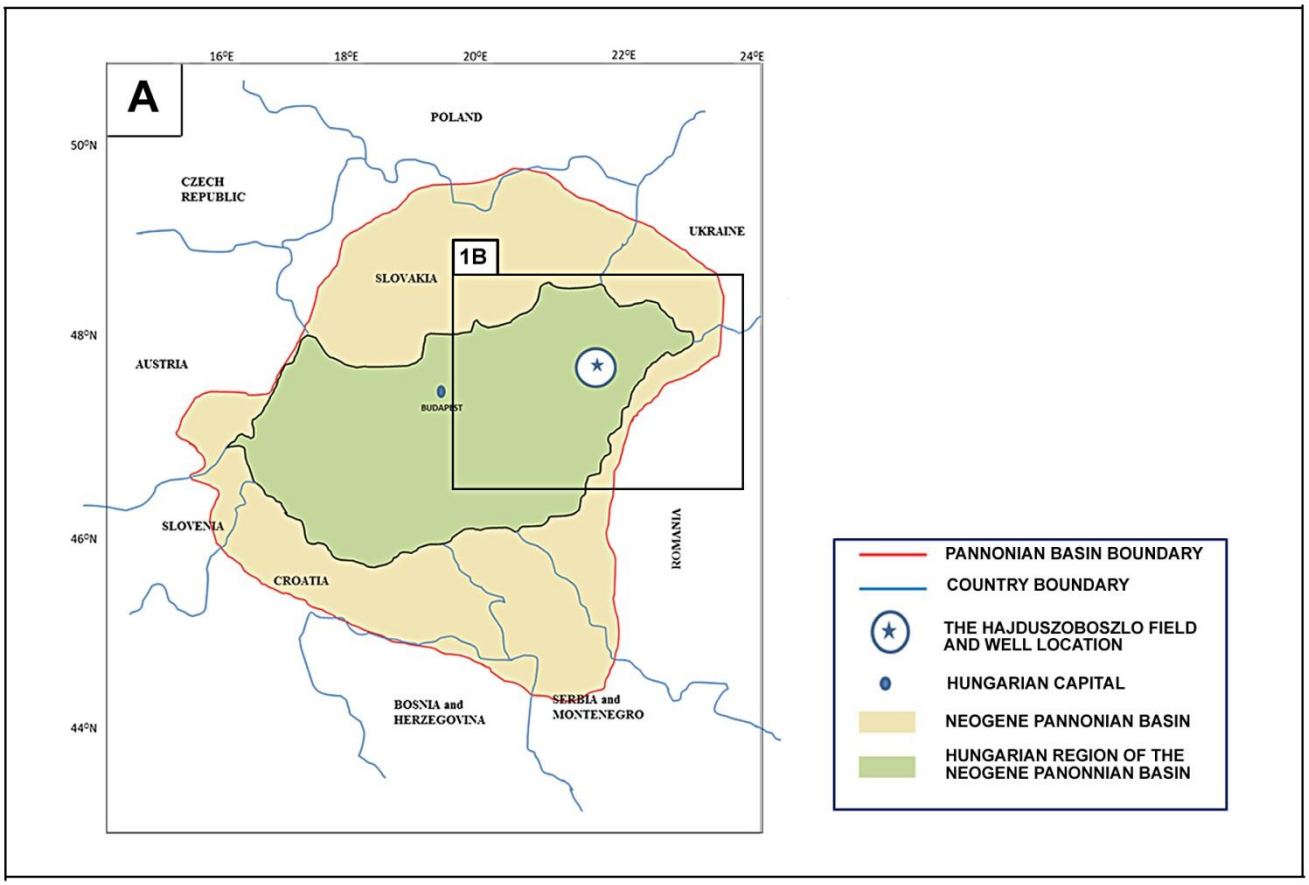

Figure 3.1(a): Map showing the Hajdúszoboszló field, well location, Hungarian region of the Pannonian Basin, and the Neogene Pannonian Basin.

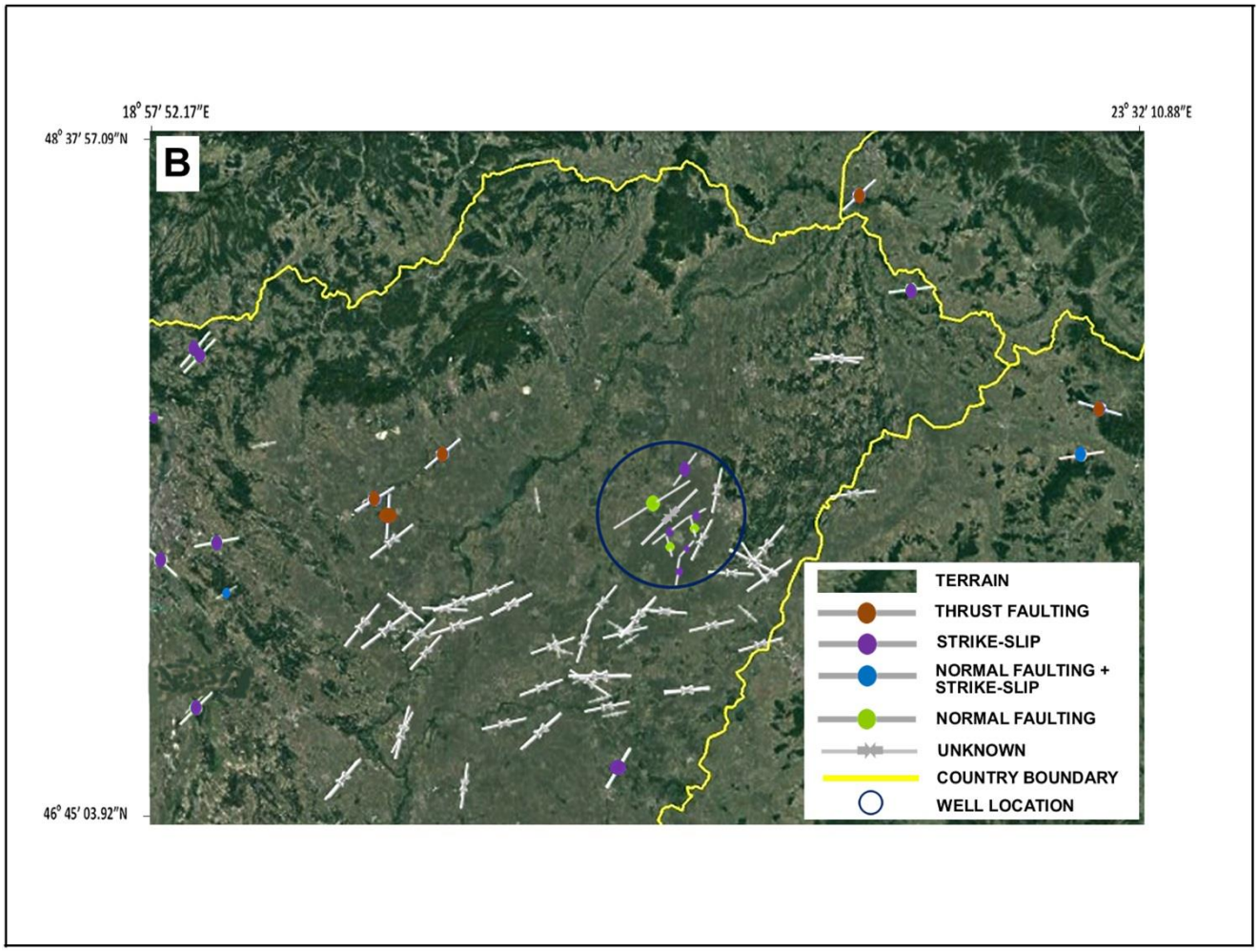

Figure 3.1(b): Google earth map of North-Eastern Hungary showing maximum horizontal stress direction (Solid-Grey lines), modified after Heidbach et al., 2016.

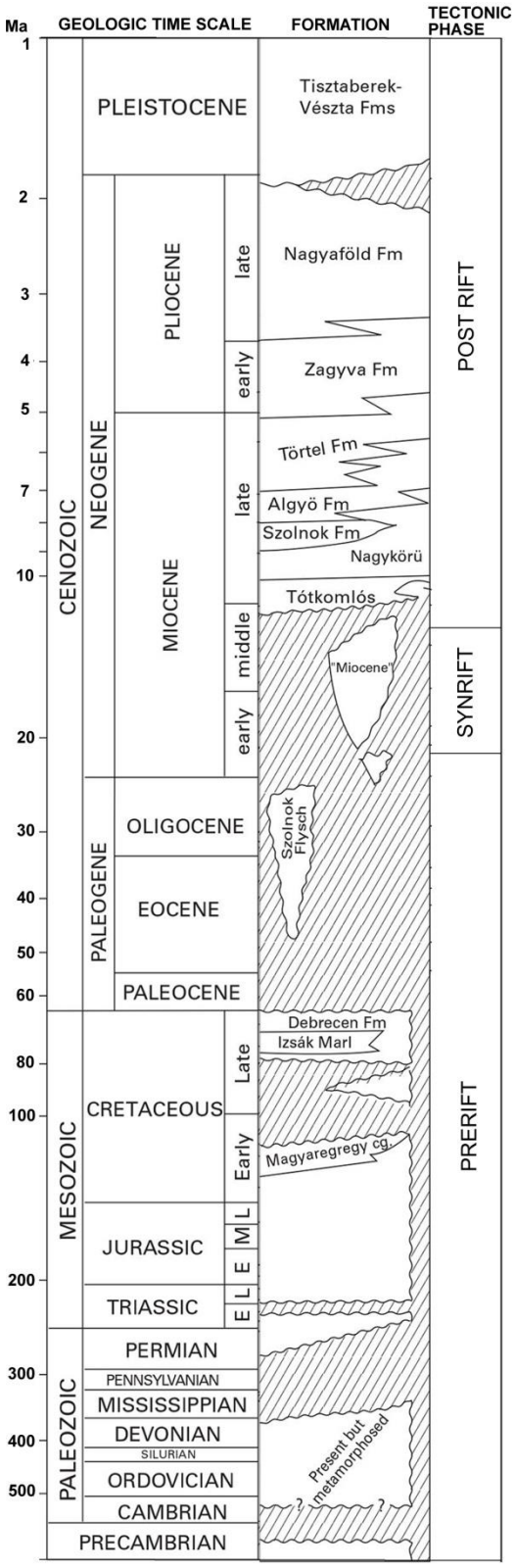

Figure 3.2: Stratigraphic column of Great Hungarian Plain in the Neogene Pannonian Basin province. Modified after Dolton, 2006.

In a severe and high-risk drilling environment, other known conventional approaches to provide solutions to the wellbore failure problems did not work (Plumb, 2000). Sand flow test is often employed to detect and measure sand production on surface during drill stem test [DST]. For us to accurately predict sand production potential, detailed information about the rock mechanical strength, the in-situ earth stresses, and the way the rock will fail is required. Although rock strength data may be obtained from laboratory measurements of recovered core samples, but information about the rock mechanical properties of all the zones in the reservoir cannot not be directly determined from this measurement (Carlson et al., 1992). The core may also be significantly altered during the journey from wellbore to laboratory.

In order to predict these weak intervals where the wellbore will fail and also the depths at which sand is likely to be produced into the wellbore, I analyze the geomechanics of reservoir formations within the wellbore. I utilized petrophysical log data from gas well HSZ-197 in Hajdúszoboszló field located in the Pannonian Basin, to use a Mechanical Earth Model (MEM) (Plumb et al., 2000; Acock et al., 2004; Lee et al., 2009; Mohiuddin et al., 2009; Qiuguo et al., 2013; Subbiah et al., 2014; Groot et al., 2014) to explore the wellbore instability and sand production boundaries in the well from surface to bottom of the well (0-965 m). The newly-released version of Schlumberger Techlog™ 2017 was available and used to test this methodology.

3.2. Mechanical Earth Model (MEM):

A Mechanical Earth Model (MEM) is an explicit description of the geomechanical properties of the reservoir and overburden formations relevant to well construction that includes the pore pressure, state of in-situ stress, and mechanical rock properties as a function of depth for the stratigraphic sections penetrated by well (Mohiuddin et al., 2009; Subbiah et al., 2014).

I adopted MEM as the foundation for our geomechanical wellbore stability analysis and sand management analysis study. In the work flow chart (Figure 3), I used to construct and calibrate our geomechanical model, the most important input data are Gamma Ray and density logs, in addition to compressional slowness (DTC) and shear slowness logs (DTS).

I used Gamma Ray log to create the mechanical stratigraphy because lithological variations in MEM parameters are governed by the mechanical stratigraphy, and the Gamma ray logs best indicates sandstone and shale formations. Overburden stress can be obtained from

density log, and the pore pressure profile can also be obtained from the sonic log data (DTS and DTC).

The description of the formation lithology is the first step of the MEM work flow. The mechanical responses and properties of grain-supported and clay-supported formations differ from one another. Therefore, classifying rocks according to their mechanical stratigraphy makes it possible for me to apply different correlations and relations to best estimate the reservoir geomechanical properties.

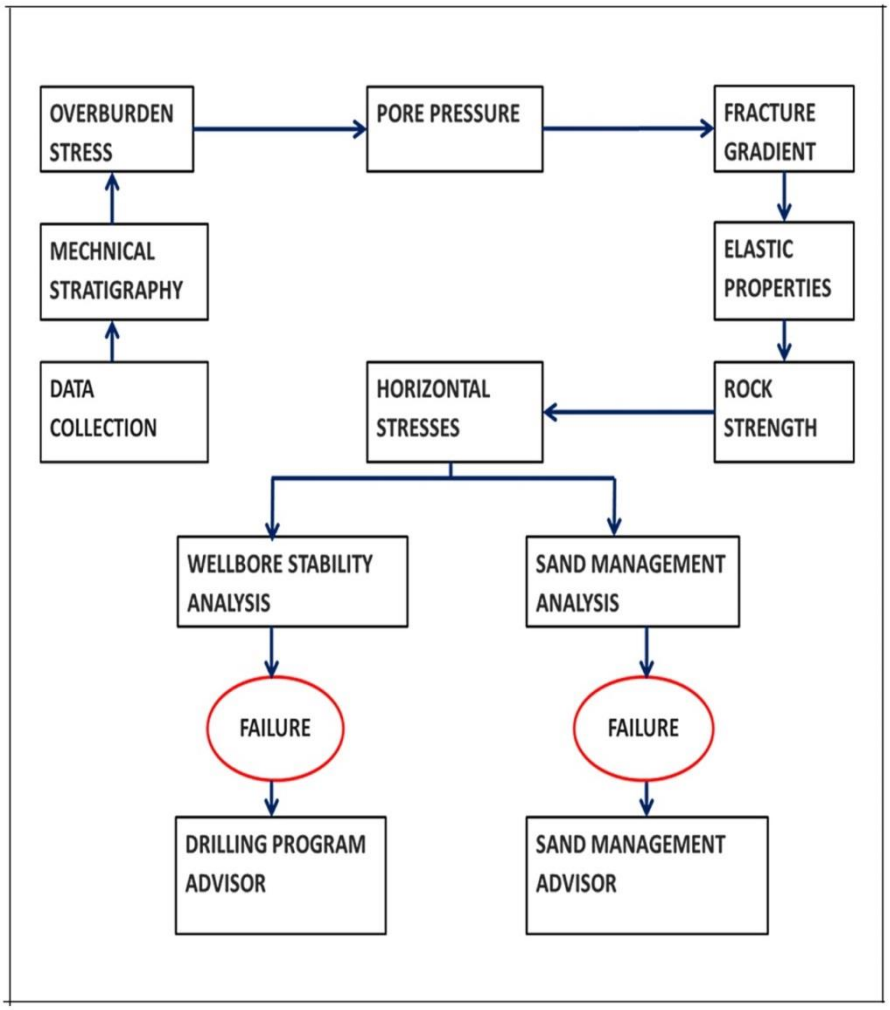

Figure 3.3: Workflow chart illustrating 1-D MEM of wellbore instability and sand production prediction.

Three of the greatest challenges in building the MEM include (Plumb, 2000):

a) Data acquisition from a wide range of disciplines (from drilling engineers, exploration geologists, mud loggers, reservoir engineers etc.).

b) Data management and organization, and the data processing.

c) Interpretation time.

3.3. Overburden Stress:

This is the pressure exerted by the weight of the overlying sediments at any given depth. In most sedimentary basins, the overburden stress is also known as Vertical stress. The density is useful for determining mechanical properties in two manners: first, the density is needed to convert from acoustic velocities to dynamic elastic moduli. Second, the density integrated over the vertical depth of the well is usually considered to give a good estimate of the vertical stress, at least in areas of low tectonic activity.

When the density log is available, the problem of determining the full in-situ stress field is then reduced to determining the magnitude and orientation of the horizontal stresses. However, the density log is rarely available in the first few hundred meters of a well. Then it is necessary to make estimates of the density to obtain the total vertical stress.

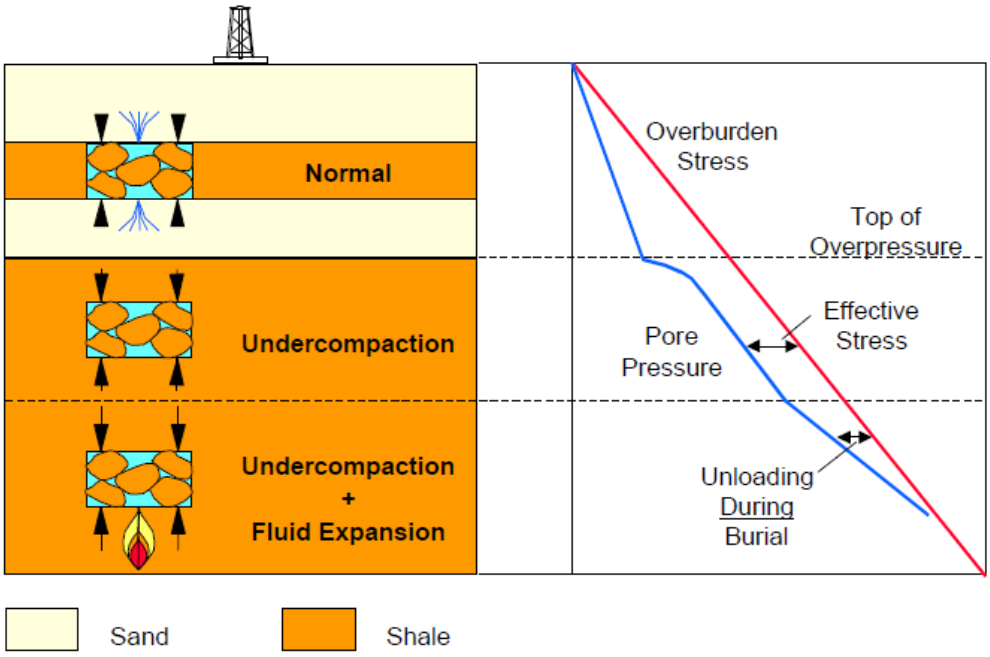

Figure 3.4: The response of Rock Effective Stress to different Overpressure Mechanisms

Density log is used to evaluate the overburden stress, since the densities of the overlying

sediments are known. Then, the overburden stress is estimated from the bulk density and formation temperature; and the resultant density curve is then integrated from top to bottom of the well.

$$\sigma_v = g \int_0^{TVD} \rho_b\ (z)dz \tag{8}$$

Where:

σ_v - Overburden stress at depth TVD (psi)

ρ_b – Bulk density (lb/ft^3)

g – Gravitational constant

3.4. Pore Pressure and Fracture Gradient:

Pore pressure is an important component for stress analysis and MEM creation. Underpinning pore pressure interpretation is the vertical effective stress equation for porous media based on Terzhagi Law. The Terzhagi's Law is given as:

$$\sigma'_v = \sigma_v - \alpha P_p \tag{9}$$

Where:

σ'_v - Vertical effective stress (psi)

σ_v – Overburden stress (psi)

P_p – Pore pressure (psi)

α – Biot coefficient (usually assumed to be 1 for shale)

Normal pore pressure is estimated for shale formation with linear method using compressional slowness (DTC), overburden stress and mechanical stratigraphy flag for shale.

$$PPnormal = PP_o + K.Z \tag{10}$$

Where:

Z – True vertical depth (TVD) (ft)

PP_o – Pressure at sea floor (psi)

K – Constant gradient (psi/ft)

The rock fracture gradient can also be estimated using the EATON method, from the pore pressure and overburden pressure and effective Poison's ratio.

Fracture gradient formula used:

$$FG = K * (\sigma_v - \alpha P_p) + \alpha P_P \quad (11)$$

$$K = \upsilon/(1-\upsilon) \quad (12)$$

Where:

α – Biot coefficient

K – Stress ratio (unitless) (It is the ratio of horizontal effective matrix stress to the effective vertical stress).

υ – Effective Poisson ratio in shale (0.25)

3.5. Elastic Properties:

The rock elastic properties are important in estimating rock strength and in-situ stresses. The rock elastic properties we obtain from petrophysical logs are known as elastic dynamic properties, because the measurements from sonic logs were conducted at high frequencies.

Wellbore failure is a relative slow process when compared to the sonic log measured at high frequency, and as a result, the dynamic elastic properties obtained from petrophysical logs are then calibrated against static measurements. The rock elastic properties is estimated using bulk density log, compressional slowness (DTC), and shear slowness (DTS), while assuming homogenous, elastic and isotropic formation.

The elastic dynamic properties are estimated as follows:

$$G_{dyn} = (13474.45)\frac{\rho_b}{(\Delta t_{shear})^2} \quad (13)$$

$$K_{dyn} = (13474.45)\rho_b\left[\frac{1}{(\Delta t_{comp})^2}\right] - \frac{4}{3}G_{dyn} \quad (14)$$

$$E_{dyn} = \frac{9G_{dyn} \times K_{dyn}}{G_{dyn} + 3K_{dyn}} \quad (15)$$

Where:

ρ_b – Bulk density of the formation (lb/ft^3)

Δt_{shear} – Shear slowness of the bulk formation (μs/ft)

Δt_{comp} – Compressional slowness of the bulk formation (μs/ft)

G_{dyn} - Dynamic shear modulus (Mpsi)

K_{dyn} - Dynamic bulk modulus (Mpsi)

E_{dyn} - Dynamic Young's modulus (Mpsi)

The John Fuller correlation (Chang et al., 2006) is introduced to derive elastic static properties because it is applicable to both sandstone and shale formations as our reservoir.

Estimated Biot elastic coefficient (α) (Klimentos, 2006) is also introduced to the model because, it aids a more accurate determination of critical drawdown pressures below which we can expect sand production to occur in a rock-failure and sand production prediction models.

3.6. Rock Strength:

Rock strength is the ability of the rock to withstand in-situ stress environment around the wellbore. A common determinant of rock strength is the unconfined compressive strength (UCS) which we estimate from the Young's modulus, and Poisson Ratio. These is used to determine wellbore failure during drilling, and also sand failure due to formation pressure drawdown because, it is the maximum stress that can be exerted on the rock before it experiences failure (Subbiah, 2014).

We also estimate the internal friction angle of a rock to determine the failure envelope of the rock when applying the Mohr-Coulomb Failure Criteria (Coates and Denoo, 1981; Subbiah,

2014). When a rock material falls under tension, the ability of the rock to withstand tensile failure is determined, and this is known as the rock tensile strength; which is useful in stability analysis of the rock.

$$UCS = 0.0866 \times \frac{E_{dyn}}{C_{dyn}} \left(0.008V_{sh} + 0.0045(1 - V_{sh})\right) \quad (16)$$

$$C_{dyn} = \frac{1}{K_{dyn}} \quad (17)$$

Where:

UCS - Unconfined Compressive Strength (Mpsi)

E_{dyn} – Dynamic Young's Modulus (Mpsi)

K_{dyn} – Dynamic Bulk Modulus (Mpsi)

C_{dyn} – Dynamic Bulk Compressibility (1/Mpsi)

V_{sh} – Shale/clay volume (ft^3/ft^3)

3.7. Horizontal Stresses:

The horizontal stress is also important in wellbore and sand management analysis model. We calculate the minimum and maximum horizontal stresses to compute the failure analysis based on assumption that the overburden (vertical) stress is the principal stress.

The minimum horizontal stress is estimated to describe the boundary for the mud loss. We also adopted the Poro-elastic horizontal strain model (Bradford and Cook, 1994; Van Den Hoek, 1996) to estimate the in-situ horizontal stresses, because rock with higher Young's modulus supports higher horizontal stress.

In using MEM, we also account for situations where sandstones are under higher horizontal stress than adjacent shale. We use Poisson Ratio, Young's modulus, overburden stress, pore pressure and Biot coefficient (α) in the estimation of horizontal stress parameters.

$$\sigma_h = \frac{V}{1-\upsilon}\sigma_V - \frac{V}{1-\upsilon}\alpha P_p + \alpha P_p + \frac{E}{1-V^2}\varepsilon_h + \frac{\upsilon E}{1-V^2}\varepsilon_H \quad (18)$$

$$\sigma_H = \frac{V}{1-\upsilon}\sigma_V - \frac{V}{1-\upsilon}\alpha P_p + \alpha P_p + \frac{E}{1-V^2}\varepsilon_H + \frac{\upsilon E}{1-V^2}\varepsilon_h \quad (19)$$

Where:

σ_h – Minimum horizontal stress (psi)

σ_H – Maximum stress (psi)

ε_h – Minimum principal horizontal strain (-)

ε_H - Maximum principal horizontal strain (-)

σ_v – Total vertical stress (psi)

P_p – Pore pressure (psi)

α – Biot elastic constant (-)

υ – Poisson ratio (-)

3.8. Wellbore Stability Analysis:

During wellbore drilling operation stresses are generated and spread around the surrounding well, this causes the wall of the borehole shear strength to exceed its threshold, and result in stress-induced wellbore failure. Wellbore instability is caused by tensile or shear failure.

We can estimate the shear failure with the Mohr-Coulomb criteria, while tensile failure is estimated at the point where the borehole tensile hoop stress exceeds the rock tensile strength. For the wellbore stability analysis of the reservoir, single-depth sensitivity analysis and wellbore failure image prediction are conducted using the already estimated pore pressure, rock elastic properties, rock strength and horizontal stresses.

The wellbore stability analysis is based on the following assumptions:

- Using Mohr-Coulomb failure criterion
- No borehole deviation or bore hole azimuth, because it is a vertical well

- There is failure image prediction, and the failure image has zero degree reference (from top of the borehole).
- No casing at casing shoe depths
- Shallow well

From the 1-D MEM wellbore stability analysis results, I can observe and identify the high-risk zones where there is high possibility of mud loss, high breakdown pressure, mud kick and shear failure in the formation.

3.9. Sand Management Analysis:

The 1-D MEM sand management analysis is used to analyze and predict fluid production rates (critical drawdown pressure), while avoiding the damage and production of weakly-consolidated sands into the near-borehole. In the analysis, I take to consideration the stress analysis and failure prediction around the wellbore (perforation or open hole) as the most viable starting point.

For the sanding analysis, already estimated Poisson ratio, rock strength (UCS), pore pressure, and horizontal stresses) are used to predict the high-risk depth interval where sanding is likely to occur. In the sand failure prediction, I also observed how the critical drawdown pressure (CDDP) changes might occur for a perforation completion over the life of the Hajdúszoboszló field, Pannonian basin, as it undergoes depletion.

I further developed a plot to represent the sand potential prediction, which represents the critical bottom-hole flowing pressure (BHFP) as a function of the reservoir pressure for a single-depth which is suspected as weakest point in the perforated interval.

CHAPTER 4

Results and Discussion

4.1. Mechanical Stratigraphy of Hajdúszoboszló Field:

Mechanical stratigraphy is created for our investigated HSZ-197 well in the Hajdúszoboszló field, Pannonian Basin, Hungary. The result (Figure 4.1) show the shale and sandstone distribution in the formation. The sandstone interval is at 150-550 m, but at an interval of 550-937.4 m, there is interbedded sand stone and shale formation.

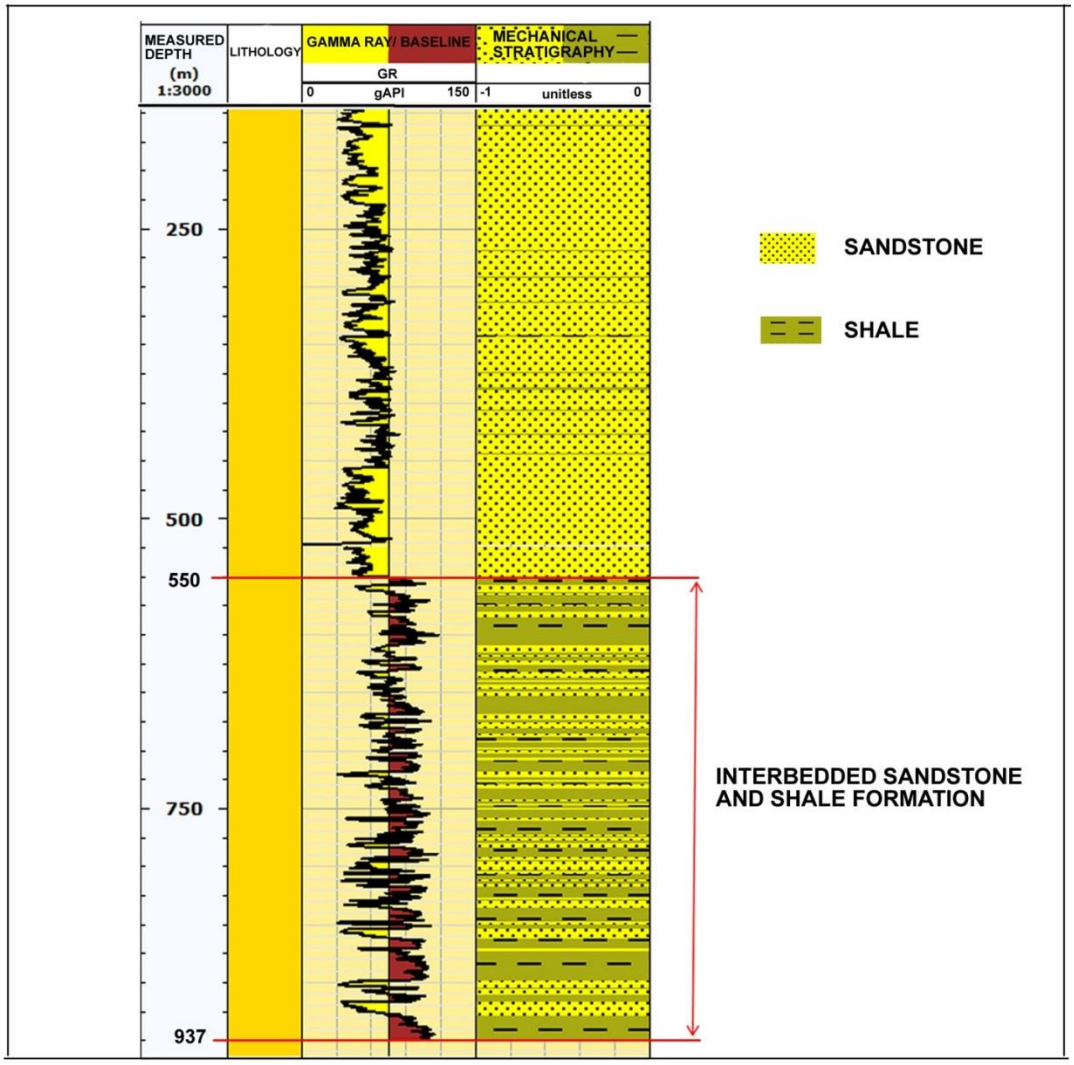

Figure 4.1: Mechanical stratigraphy result showing the sandstone and shale distribution in Hajdúszoboszló field, Pannonian Basin, Hungary.

4.2. Wellbore Instability in Hajdúszoboszló Field:

The results obtained for estimated overburden stress, pore pressure, rock fracture gradient, Young's modulus (static and dynamic), shear modulus (static and dynamic), bulk modulus (static and dynamic), and poison ratio (static and dynamic). The Biot elastic coefficient (α) estimated is between 0.2493–1.00 at an interval of 56.0- 941.0 m. Table 1 shows the result for the overburden stress, pore pressure, unconfined compressive strength (UCS), tensile strength, and horizontal stresses at various depths. The result of the 1-D MEM wellbore stability analysis (Table 2) shows: mud weight profile (Figure 4.2); while potential wellbore shear and tensile failures, and also the breakout and breakdown pressures are shown in Figure 4.3a. The shallow knockout and wide breakout interval is shown Figure 4.3b, while Figure 4.4 shows the wellbore sensitivity analysis.

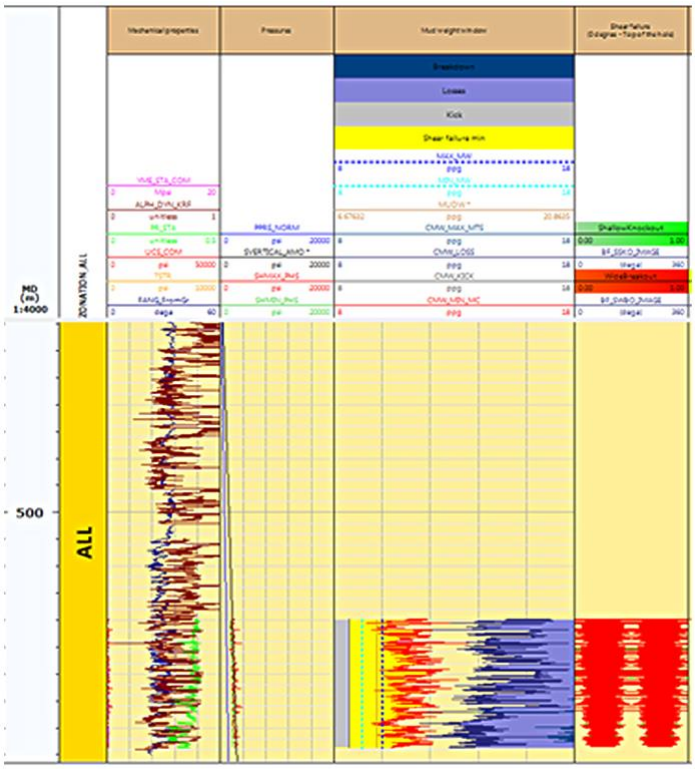

Figure 4.2: 1-D MEM Wellbore Stability Analysis result showing mud weight profile for the entire well depth from top to bottom.

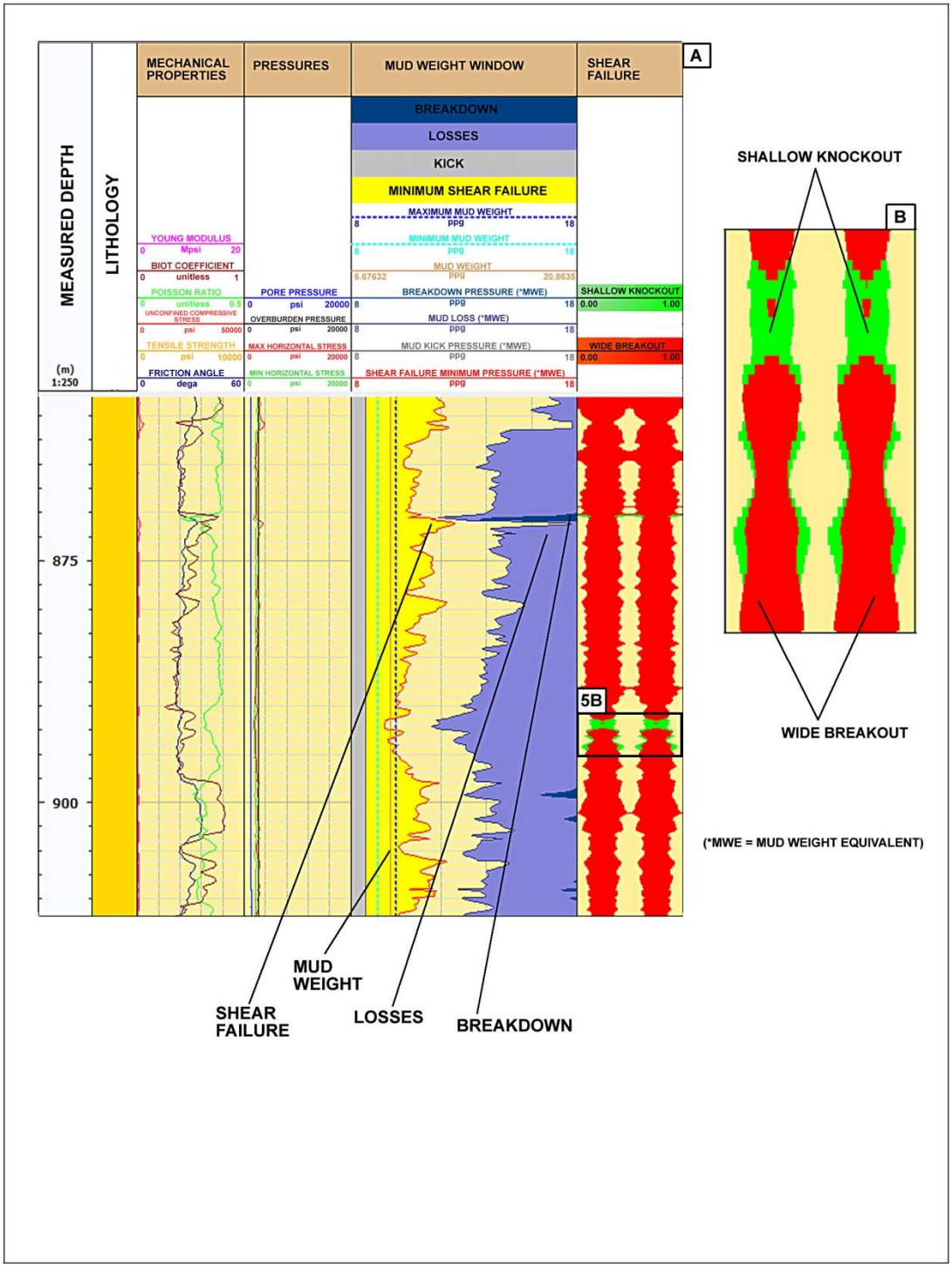

Figure 4.3: (a) 1-D MEM wellbore stability analysis illustrating shear and tensile failures; breakdown and breakout pressures. (b) Formation cross-section showing wellbore breakouts and shallow knockout.

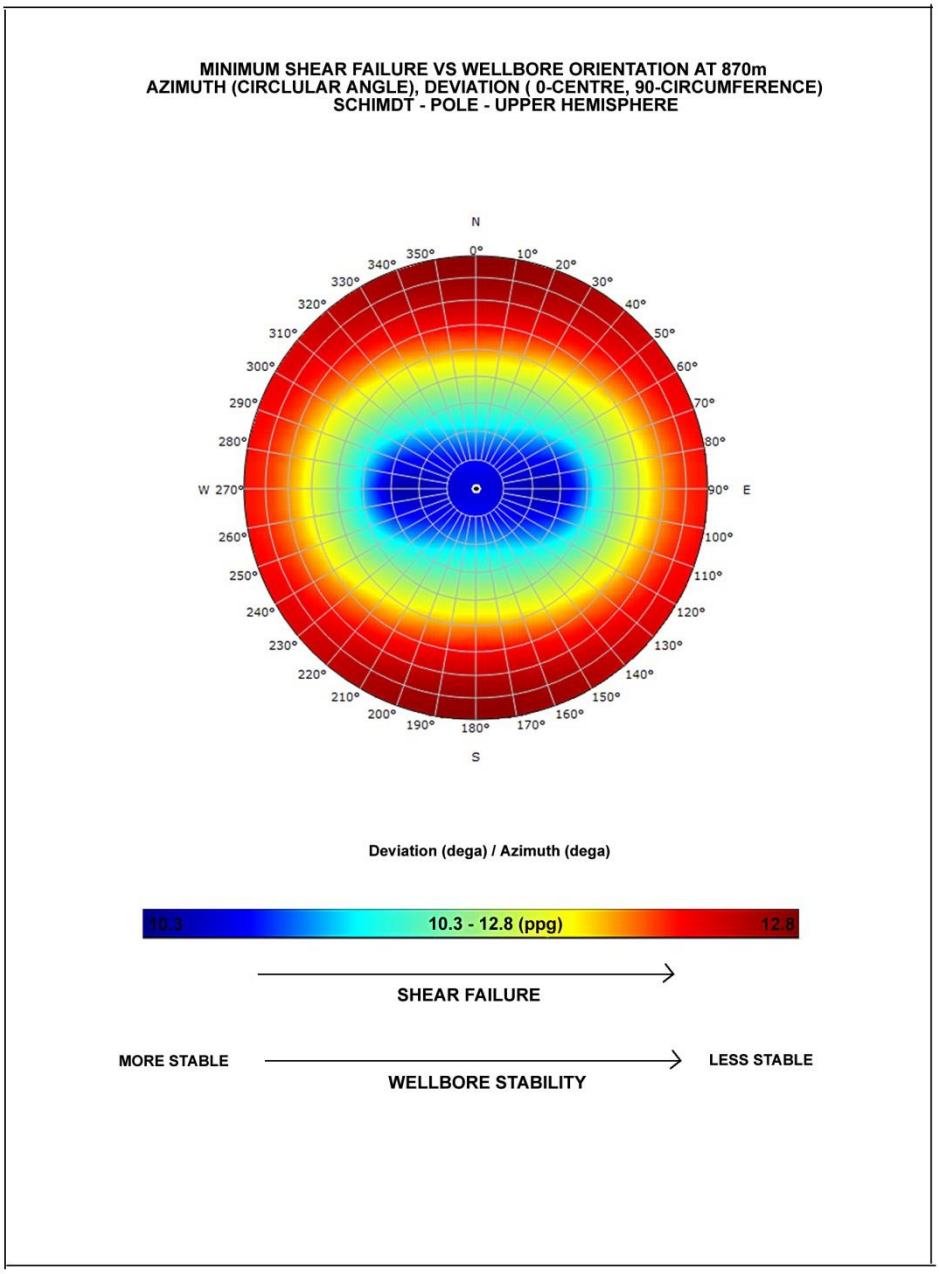

Figure 4.4: Wellbore sensitivity analysis result illustrating shear failure minimum mud weight as a function of wellbore orientation at a single depth.

TABLE 4.1: MEM Result for HSZ-97 Well Located In Hadjuszoboszlo Field, Pannonian Basin, Hungary

WELL DEPTH	OVERBURDEN /VERTICAL STRESS	PORE PRESSURE	UNCONFINED COMPRESSIVE STRENGTH	TENSILE STRENGTH	MAXIMUM HORIZONTAL STRESS	MINIMUM HORIZONTAL STRESS
(m)	(psi)	(psi)	(psi)	(psi)	(psi)	(psi)
0.0	0	0	-	-	-	-
0.1	0.2981	0.1476	-	-	-	-
150.0	447.8454	221.3928	-	-	-	-
300.0	898.0070	442.7855	-	-	-	-
500.0	1503.5860	737.9759	-	-	-	-
698.6	2112.5930	1031.1000	897.18	89.7181	2381.7910	2022.6170
700.0	2116.9170	1033.1660	683.82	68.3816	2316.1350	1994.1930
800.0	2426.9550	1180.7610	731.25	73.1252	2629.395	2256.8720
860.6	2616.0290	1270.204	1889.45	188.945	3484.7230	2661.3480
870.0	2645.4400	1284.078	301.80	30.1800	2293.2310	2087.1830
900	2739.4600	1328.3570	569.96	56.9962	2699.1770	2242.9860
937.4	2857.0020	1383.5600	417.48	41.7480	2502.8820	2214.2980
965.0	2943.9850	1424.2900	-	-	-	-

4.3. Sand Production in Hajdúszoboszló Field:

The 1-D MEM sand management analysis used to predict sand production potential in the Hajdúszoboszló field, show the sanding interval analysis results (Fig. 4.5) at 0%, 0.3%, 15%, 25% and 35% depletion rates for perforation completions. The sanding single-depth analysis result at 860.6 m (Fig. 4.6) shows the sand-free and sand failure zones.

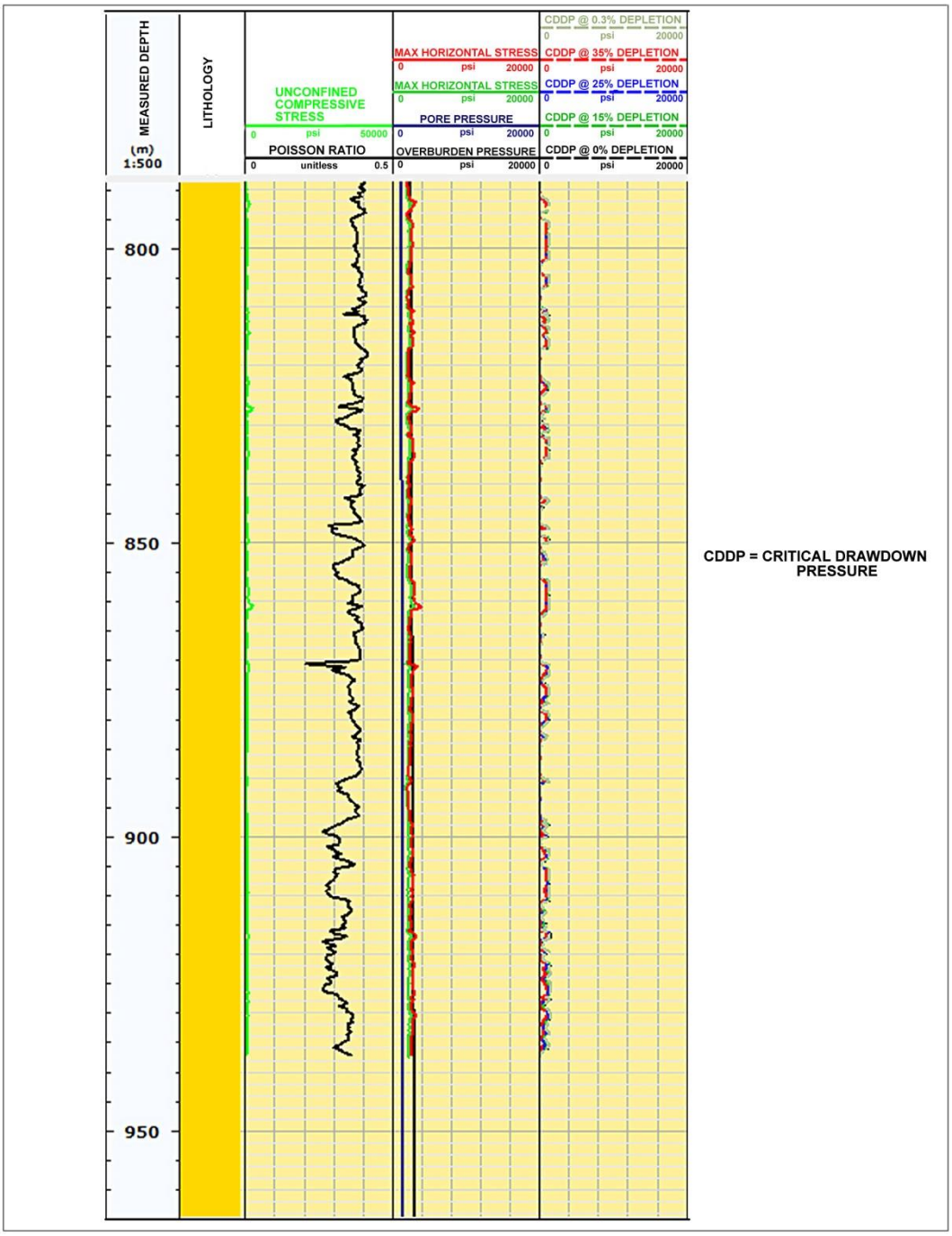

Figure 4.5: Sanding interval analysis illustrating the sanding risk for the perforated well as a function of depletion.

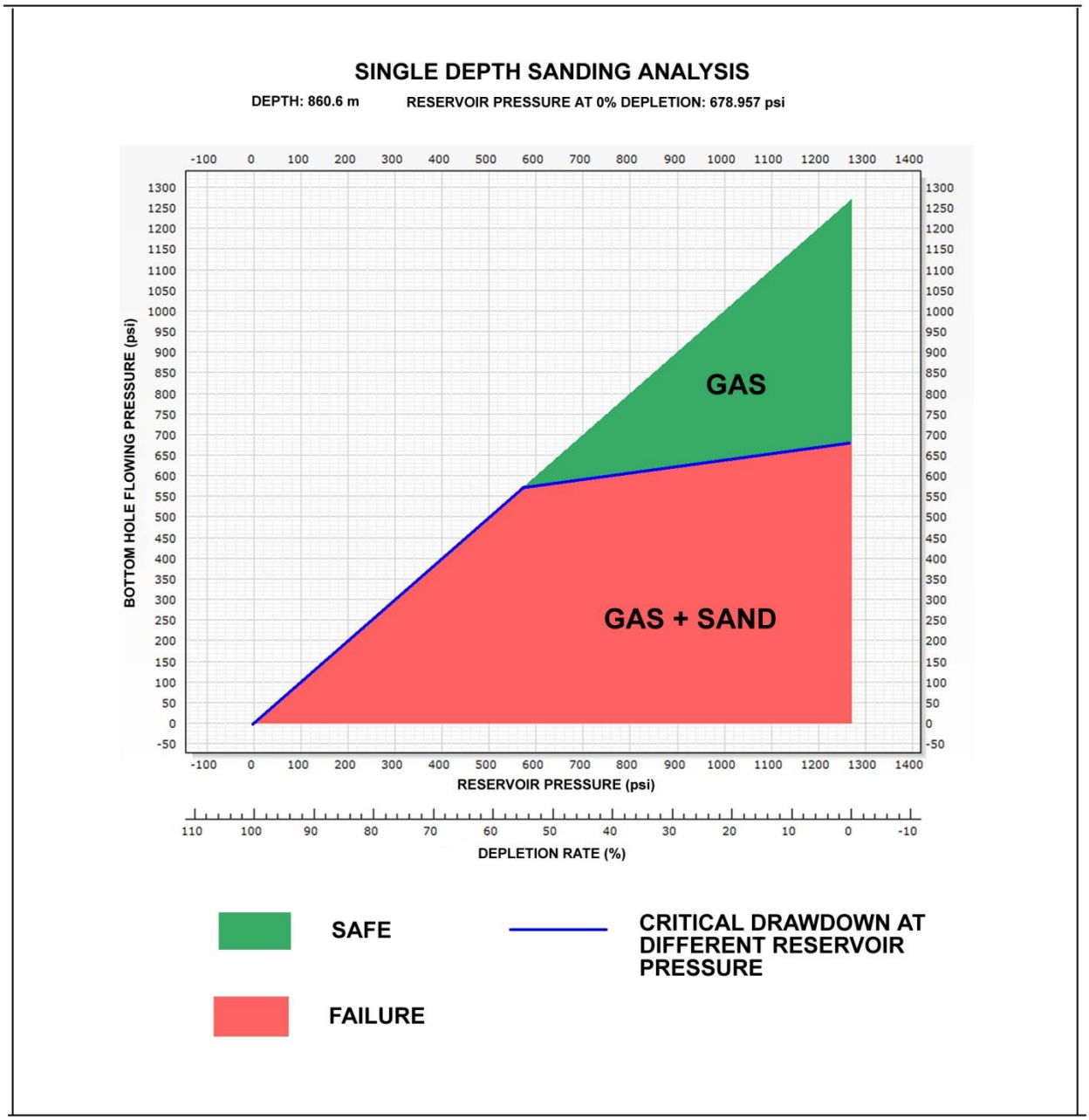

Figure 4.6: Sanding single depth analysis result illustrating critical drawdown pressures, sand-free and sand failure zones.

4.4. Discussion:

From the mechanical stratigraphy result of the HSZ-197 well (Figure 4.1), the reservoir consists of mainly sandstone at an interval of 150-550 m. But beyond this depth, an interval in the reservoir (550-937.4 m) is identified with interbedded sandstone and shale formation. This formation interval is mostly composed of shale with non-uniform layers of sandstone rocks fragments. From the observation, this interval is weak, unconsolidated, and have poor cementation. Significant overpressure and abnormally high in-situ temperature conditions can be expected at this interval (550-937.4 m), and as a result, wellbore instability and sand production can be expected to occur at this formation interval.

From Table 1, the wellbore stresses is observed start to propagate at a depth of 698.6 m (2292 ft) and in addition, the formation stress distribution is evident at depth interval of 698.6-937.4 m (2292-3075.46 ft). The estimated overburden pressure, pore pressure, and the minimum and maximum horizontal stresses in the wellbore are observed also be significant at this depth interval (698.6-937.4 m). As a result, wellbore instability is expected to occur at this formation interval.

Figures 4.2-4.3 and Table 2 shows another result of the wellbore stability analysis through the wellbore failure prediction images. A wellbore depth interval of 698.6-937.4 m (2292 ft) is observed as a high-risk zone characterized by significant shear failure, mud losses, and high pressure breakdown (tensile failure). Also, the wellbore is observed to attain its maximal value of shear failure, breakdown, and mud loss at a depth interval between 870-875 m. In Figure 4.3b, a wide breakout is observed in the wellbore at the same interval of 698.6-937.4 m, while the shallow knockout is most prominent at depth interval of 890-900 m. At this interval, stress-induced enlargement is experienced in the wellbore. When the pressure in the borehole (mud weight) does not counterbalance the pressure in the permeable formation, there is uncontrolled inflow of formation fluid into the wellbore. The wellbore stresses at this interval (698.6-937.4 m) will tend to re-open the natural fractures around the wellbore, and hence cause mud loss into the formation at this zone. These suggest high possibility of wellbore instability at this formation interval.

The result of the sensitivity analysis conducted at selected depth of 870 m (2854.3 ft) in Figure 4.4 shows the shear failure minimum mud weight (breakout) as a function of borehole orientation. From the result, the maximum horizontal stress (σ_H) is observed to be acting around

the wellbore region of the northeast-southwest and northwest-southeast orientation. The color shades indicates the wellbore damage mud weight. The wall of the wellbore (Figure 4.4) with the highest shade of red color indicates the maximum shear failure at this depth tending towards the maximal value of 1533.8 kg/m^3 (12.8 ppg). This maximum shear failure around the region is observed to be perpendicular to the maximum horizontal stress, and this region gives the breakout width. Due to the high stress concentration around the wellbore at this region and depth, a significant mud loss and a large breakout width is expected. These also confirm a high possibility of wellbore instability at this formation depth.

The difference between the reservoir pressure and the bottom-hole flowing pressure gives the drawdown pressure (DDP). Figure 4.5 illustrates the result of the sanding interval analysis, and how the critical drawdown pressure (CDDP) changes for perforation completion as the wellbore undergoes depletion at various rates (0%, 0.3%, 15%, 25%, 35%). This shows the result of sanding risk for the perforated well as a function of depletion across the investigated interval (0-965 m). A high possibility of solids is observed to be produced into the formation at an interval of 698.6-937.4 m (2292-3075.46 ft), and as a result, there is high sanding potential at this formation interval.

Sanding single depth analysis result (Figure 4.6), shows the plot of the bottom-hole flowing pressure (BHFP) against the reservoir pressure at borehole depth of 860.6 m (2823.49 ft). The reservoir pressure is represented on the abscissa axis, while the bottom-hole flowing pressure is represented on the ordinate axis, and the changes are observed with reservoir depletion. The critical drawdown at different reservoir pressure (blue line) is illustrated with the boundary between green region and the red region. Also, the reservoir pressure where there is zero depletion (0%) is at 46.81 bar (678.96 psi). As the reservoir pressure is continuously depleted, the drawdown pressure decreases, and results in a negative critical drawdown pressure (CDDP). Therefore, since the expected applied drawdown pressure (DPP) is above the CDDP, there is high risk of sand production in the weak intervals of the reservoir.

From observations, the green region indicates the reservoir pressures for which no sanding is expected and this well can be produced without sand (safe zone). On the other hand, the red region indicates the reservoir pressures for which sand production is expected and this gas well in the Hajdúszoboszló field will experience sand production (failure zone). This is the weakest point in the formation interval and also with the highest potential for sand production.

These also confirm the existence of sand production risk at this formation interval in the Hajdúszoboszló field.

The absence of downhole validation tools for this study means that the reservoir may not always experience wellbore instability, and also not always produce sand at the predicted zones. However, succession of work done on wellbore stability and sand production prediction using the 1-D MEM combined with petrophysical log data supports the possibility of sand production and wellbore instability in the predicted depth intervals in the Hajdúszoboszló field, Pannonian basin., Hungary.

CHAPTER 5

Conclusions and Recommendations

A 1-D MEM developed by Schlumberger Techlog™ 2017 is used to estimate, predict and quantify wellbore instability and sanding potentials in Hajdúszoboszló field located in eastern part of Pannonian basin, Hungary.

The observations from results of the 1-D MEM wellbore and sanding analysis in the Hajdúszoboszló field, Pannonian basin, Hungary, using a shallow onshore gas well (0-965 m) suggests that:

- The formation interval of 550-937 m is characterized by weak, unconsolidated, overpressured and interbedded sandstone and shale formation.
- The depth interval of 698.6-937.4 m represents an over-pressured, unconsolidated, and highly stressed formation with a high tendency for wellbore failure during drilling process, and the Hajdúszoboszló field has a 90% possibility of wellbore instability.
- The formation interval 698.6-937.4 m provides the weakest, unconsolidated formation with high-risk sand production potential during well completion operation, and the Hajdúszoboszló field has a 70% potential of producing sand into the wellbore at this zone.

My study validates the importance of the MEM in wellbore stability analysis and also in predicting sand production potential in the Pannonian basin, which is valuable in proactive decision making during drilling and well completion operations in both a single borehole and for the entire Hajdúszoboszló field development.

Although data for 1 well was available to us at the time of this study, I recommend that in order to better validate the result of this model, there is need to include data from other wells in the Hajdúszoboszló field as well as other fields located within the Pannonian basin, Hungary.

References

1. Acock, A., ORourke, T., Shirmboh, D., Alexander, J., Anderson, G., Kaneko, T., Venkitaraman, A., Lopez-de-Cardenas, J., Nishi, M., Numasawa, M., Yoshioka, K., Roy, A., Wilson, A., and Twynam, A., (2004) "Practical approaches to sand management," Oilfield Review, pp. 10-27, Spring 2004.
2. Alliquander, O., (1970) "Aspects of deep drilling in the Carpathian Basin," Journal of Petroleum Technology, vol. 22, issue 02, February 1970.
3. Alliquander, O., and Csaba, J., (1976) "Drilling and well completion problems in geopressured formations of the Carpathian Basin," SPE 5754 presented at the SPE-European Spring Meeting, Amsterdam, Netherlands, April 8-9.
4. Al-Shaaibi, S.K., Al-Ajmi, A.M., and Al-Wahaibi, Y., (2013) "Three dimensional modeling for predicting sand production," Journal of Petroleum Science and Engineering, vol. 109, pp. 348-363.
5. Amiebenomo, H.C., and Adewale, D., (2015) "Sand control using geomechanical techniques: A case study of Niger Delta, Nigeria," International Journal of Science Inventions Today, vol. 4, issue 5, pp. 439-450.
6. Anderson, R.A., Ingram, D.S., and Zanier, A.M., (1973) "Determining Fracture Pressure Gradients from Well Logs," Journal of Petroleum Technology, pp. 1259.
7. Angelov P.V., (2009) "4D seismic reservoir characterization integrated with geo-mechanical modeling," Ph.D. Thesis, Delft University of Technology, Delft, Netherlands.
8. Bada, G., and G., Tari., 2012. Exploration Focus: Hungary. AAPG Search and Discovery article 10534, accessed December 12, 2017, http://www.searchanddiscovery.com/documents/2013/10534bada/ndx_bada.pdf
9. Bell, J.S. and Gough, D. I., (1979) "North East -South West compressive stresses in Alberta: evidence from oil wells," Earth and Planetary Science Letters," 45, pp. 475-482.
10. Bradford, I.D.R. and Cook, J.M., (1994) "A semi-analytic Elastoplastic Model for Wellbore Stability with Applications to Sanding," SPE-28070 presented at the SPE Rock Mechanics in Petroleum Engineering, Delft, Netherlands, August 29-31.
11. Bradley, W.B., (1979) "Mathematical concept – Stress cloud can predict borehole failure," Oil and Gas Journal, 19, pp. 75 – 102.
12. Carlson, J., Gurley, D., King, G., Prince-Smith, C., and Waters, F., (1992) "Sand control:

why and how," Oilfield Review, spring ed., pp. 10-27.

13. Chang, C., Zoback, M.D., and Khaksar, A., (2006) "Emperical relations between rock and physical properties in sedimentary rocks," Journal of Petroleum Science and Engineering, vol. 51, pp. 223-237.
14. Charlez, P. A., and Heugas, O., (1991) "Evaluation of optimal mud weight in soft shale levels," presented at the 32nd US Symposium on Rock Mechanics as a multidisciplinary science, Norman, Oklahoma, July 10-12.
15. Coates, G.R., and Denoo, S.A., (1981) ''Mechanical Properties Program Using Borehole Analysis and Mohr's Circle," SPWLA-1981 presented at the SPWLA 22nd Annual Logging Symposium, Mexico City, Mexico, June 23-26.
16. Dolton, G.L., (2006) "Pannonian Basin Province, Central Europe (Province 4808)—Petroleum geology, total petroleum systems, and petroleum resource assessment," U.S. Geological Survey, b2204-b_508:1-38. Accessed December 18, 2017, https://pubs.usgs.gov/bul/2204/b/pdf/b2204-b_508.pdf.
17. EI-Sayed, A-A.H (1991) "Maximum Allowable Production Rates from Open Hole Horizontal Wells", SPE 21383 presented at the SPE Middle East Oil Show, Bahrain, 16-19 November. https://doi.org/10.2118/21383-MS.
18. Fjaer, E., Holt, R.M., Horsrud, P., Raaen, A.M., and Risnes, R., (2008) "Petroleum Related Rock Mechanics," 2nd ed., Elsevier Developments in Petroleum Science.
19. Franquet, J.A., Stewart, G., Bolle, L., and Ong, S., (2005) "Log-based geomechanical characterization and sanding potential analysis on several wells drilled in Southern part of Oman," SPE 111044 presented at the SPE/PAPG Annual Technical Conference, Islamabad, Pakistan, November 28-29.
20. Groot, L.D., Graven, H., Suez, G., and Subbiah, S.K., (2014) "Innovative sand failure analysis and prediction modeling restore lost production in North Sea field," World Oil, August ed., pp. 71-76.
21. Heidbach, O., Rajabi, M., Reiter, K., Ziegler, M., (2016) "World Stress Map 2016," GFZ Data Services. http://doi.org/10.5880/WSM.2016.002.
22. Isehunwa, S.O., Ogunkunle, T.F., Onwuegbu, S.M., and Akinsete, O.O., (2017) "Prediction of sand production in gas and gas condensate wells," Journal of Petroleum and Gas Engineering, vol. 8(4), pp. 29-35. http://doi.org/10.5897/JPGE2016.0259.

23. Ispas, I., Bray, R.A., Palmer, I.D., and Higgs, N.G., (2002) "Prediction and evaluation of sanding and casing deformation in a GOM shelf well," SPE/ISRM 78236 presented at the SPE/ISRM Rock Mechanics Conference, Irving, Texas, October 20-23.
24. Klimentos, T., (2003) "NMR applications in petroleum related rock-mechanics: sand control, hydraulic fracturing, wellbore stability," SPWLA-2003-HHH presented at the SPWLA 44th Annual Logging Symposium, Galveston, Texas, June 22-25.
25. Lee, D., Singh, V., Berard, T., (2009) "Construction of a mechanical earth model and wellbore stability analysis for CO2 injection well," SPE-126624-PP presented at the SPE International Conference on CO2, Capture, Storage and Utilization, San Diego, California, USA, November 2-4.
26. Mase, G.T., and Mase, G.E., (1999) "Continuum Mechanics for Engineers," 2nd ed., CRC Press.
27. McClean, M. C. and Addis, M.A., (1990) "Wellbore stability: The effect of strength criteria on mud weight recommendations," SPE 20405 presented at the SPE Annual Technical Conference and Exhibition, New Orleans, Louisiana, September 23-26.
28. Mohiuddin, M.A., Najem, M.M., Al-Dhaferi, Y.R., Bajunaid, H.A., and Tan, C.P., (2009) "Geomechanical characterization of a sandstone reservoir in Middle East- analysis of sanding prediction and completion strategy," SPE 120049 presented at the SPE Middle East Oil & Gas Show and Conference, Kingdom of Bahrain, March 15-18.
29. Mulders, F.M.M., (2003) "Modeling of stress development and fault slip in and around a producing gas reservoir," Ph.D. Thesis, Delft University of Technology, Delft, Netherlands.
30. Papanastasiou, P., (2006) "Cavity stability prediction method for wellbores," U.S. Patent US7066019B1, Accessed December 18, 2017, https://patentimages.storage.googleapis.com/96/b4/a9/fa22a9405f4287/US7066019.pdf.
31. Perkins, T. K. and Weingarten, J. S., (1988) "Stability and Failure of Spherical Cavities in Unconsolidated Sand and Weakly Consolidated Rock," SPE 18244 presented at the SPE Annual Technical Conference and Exhibition, October 2-5, Houston, Texas. https://doi.org/10.2118/18244-MS
32. Plumb, R., Edwards, S., Pidcock, G., Lee, D., and Stacey, B., (2000) "The mechanical earth model concept and its application to high-risk well construction projects,"

IADC/SPE 59128 presented at the IADC/SPE Drilling Conference, New Orleans, Louisiana, February 23-25.

33. Plumb, R.A. and Hickman, S.H., (1985) "Stress-induced borehole elongation: a comparison between the four-arm dipmeter and the Borehole Televiewer in the Auburn geothermal well," Journal of Geophysical Research, 90, pp. 5513-5521.
34. Qiuguo, L., Zhang, X., Al-Ghammari, K., Mohsin, L., Jiroudi, F., and Rawahi, A.A, (2013) "3D geomechanical modeling, wellbore stability analysis improve field's performance," World Oil, October ed., pp. 53-61.
35. Ranalli, G. (1995) "Rheology of the Earth," 2nd ed., Chapman and Hal.
36. Ranjith, P.G., Perera, M.S.A., Perera, W.K.G., Wu, B., and Choi, S.K., (2013) "Effective parameters for sand production in unconsolidated formations: An experimental study," Journal of Petroleum Science and Engineering, vol. 105, pp. 34-42.
37. Spencer, A.J.M., (2004) "Continuum Mechanics," Dover ed., Dover Publications, New York.
38. Subbiah, S.K., Groot, L.D., and Graven, H., (2014) "An innovative approach for sand management with downhole validation," SPE 168178 presented at the SPE International Symposium and Exhibition on Formation Damage Control, Lafayette, Louisiana, February 26-28.
39. Szabo, T., (2001) "Drilling through shallow gas zones in Hungary," The Electronic Scientific Journal Oil and Gas Business, 02(2001). Accessed December 18, 2017, http://ogbus.ru/article/view/drilling-through-shallow-gas-zones-in-hungary.
40. Tiab, D., and Donaldson, E.C., (2004) "Petrophysics: Theory and Practice of Measuring Reservoir Rock and Fluid Properties," 2nd ed., Elsevier.
41. Tigrek, S., (2004) "Seismic Evidence of Tectonic Stresses: Implications for basin reconstruction," Ph.D. thesis, Delft University of Technology, Delft, Netherlands.
42. Van Den Hoek, P.J., Kooijman, A.P., De Bree, P., Kenter, C.J., Zheng, Z., and Khodaverdian, M., (1996) "Horizontal-wellbore stability and sand production in weakly consolidated sandstones," SPE 36419 presented at the SPE Annual Technical Conference and Exhibition, Denver, Colorado, October 6-9.
43. Willson, S.M., Moschovidis, Z.A., Cameron, J.R., and Palmer, I.D., (2002) "New model for predicting the Rate of sand production," SPE-78168 presented at the SPE/ISRM Rock

Mechanics Conference, Irving, Texas, October 20-23.

44. Wu, B., Mohamed, N.A., Tan, C.P., Sukahar, M.W., Hong, T.Y., Viswanathan, C., and Yee, H.V., (2006) “An integrated wellbore stability and sand production prediction study for a multi-field gas development,” SPE 101087 presented at the SPE Asia Pacific Oil & Gas Conference and Exhibition, Adelaide, Australia, September 11-13.
45. Zhou, S., and Sun, F., (2016) “Sand Production Management for Unconsolidated Sandstone Reservoirs,” 1st ed. Singapore: Wiley, ch. 1-2, pp. 12-33.
46. Zoback, M.D, Moos, D., and Mastin, L., (1985) “Well bore breakouts and in-situ stress,” Journal of Geophysical Research, 90(B7): 5523-5530. https://www.doi.org/10.1029/JB090iB07p05523.